

University of Groningen

## PET/MRI in Infection and Inflammation

Sollini, Martina; Berchiolli, Raffaella; Kirienko, Margarita; Rossi, Alexia; Glaudemans, A. W. J. M.; Slart, Riemer; Erba, Paola Anna

*Published in:*  
 Seminars in Nuclear Medicine

*DOI:*  
[10.1053/j.semnuclmed.2018.02.003](https://doi.org/10.1053/j.semnuclmed.2018.02.003)

**IMPORTANT NOTE: You are advised to consult the publisher's version (publisher's PDF) if you wish to cite from it. Please check the document version below.**

*Document Version*  
 Publisher's PDF, also known as Version of record

*Publication date:*  
 2018

[Link to publication in University of Groningen/UMCG research database](#)

*Citation for published version (APA):*

Sollini, M., Berchiolli, R., Kirienko, M., Rossi, A., Glaudemans, A. W. J. M., Slart, R., & Erba, P. A. (2018). PET/MRI in Infection and Inflammation. *Seminars in Nuclear Medicine*, 48(3), 225-241.  
<https://doi.org/10.1053/j.semnuclmed.2018.02.003>

### Copyright

Other than for strictly personal use, it is not permitted to download or to forward/distribute the text or part of it without the consent of the author(s) and/or copyright holder(s), unless the work is under an open content license (like Creative Commons).

The publication may also be distributed here under the terms of Article 25fa of the Dutch Copyright Act, indicated by the "Taverne" license. More information can be found on the University of Groningen website: <https://www.rug.nl/library/open-access/self-archiving-pure/taverne-amendment>.

### Take-down policy

If you believe that this document breaches copyright please contact us providing details, and we will remove access to the work immediately and investigate your claim.

*Downloaded from the University of Groningen/UMCG research database (Pure): <http://www.rug.nl/research/portal>. For technical reasons the number of authors shown on this cover page is limited to 10 maximum.*

# PET/MRI in Infection and Inflammation



Martina Sollini, MD,\* Raffaella Berchiolli, MD,† Margarita Kirienko, MD,\*  
Alexia Rossi, MD, PhD,\* A.W.J.M. Glaudemans, MD, PhD,‡ Riemer Slart, MD, PhD,\*§  
and Paola Anna Erba, MD, PhD||

Hybrid positron emission tomography/magnetic resonance imaging (PET/MR) systems are now more and more available for clinical use. PET/MR combines the unique features of MR including excellent soft tissue contrast, diffusion-weighted imaging, dynamic contrast-enhanced imaging, fMRI and other specialized sequences as well as MR spectroscopy with the quantitative physiologic information that is provided by PET. Most of the evidence of the potential clinical utility of PET/MRI is available for neuroimaging. Other areas, where PET/MR can play a larger role include head and neck, upper abdominal, and pelvic tumours. Although the role of PET/MR in infection and inflammation of the cardiovascular system and in musculoskeletal applications are promising, these areas of clinical investigation are still in the early phase and it may be a little longer before these areas reach their full potential in clinical practice. In this review, we outline the potential of hybrid PET/MR for imaging infection and inflammation. A background to the main radiopharmaceuticals and some technical considerations are also included.

Semin Nucl Med 48:225–241 © 2018 Published by Elsevier Inc.

## Introduction

Positron emission tomography (PET) developed in the 1970s, was implemented in clinical practice in the late 1980s and early 1990s.<sup>1,2</sup> Hybrid PET/computed tomography (PET/CT) imaging systems were developed with the aim of utilizing high-resolution CT for attenuation correction purposes as well as for anatomical localization of the molecular information provided by PET. The development of hybrid PET/magnetic resonance imaging (PET/MR) systems has been far slower than the development of PET/CT. This has been mainly due to technical issues related to electromagnetic interference, leading to artifacts and signal-to-noise reduction in the PET or MR images.<sup>3</sup> Therefore, MR-compatible PET scanners were developed based on fiberoptic coupling of the

scintillator and the photodetectors<sup>4</sup> or the replacement of photomultiplier technology with magnetic field Y-insensitive avalanche photodiodes or silicon photomultipliers.<sup>5–7</sup> A PET/MR system capable of concurrent dynamic PET and MR scanning allowing the use of MR information for dynamic motion correction during PET data acquisition has been introduced recently.<sup>3,7</sup> In addition to the technical consideration, equipment costs, operational costs and related logistics probably also account for the slow adoption of the method; from 2010, only about 70 systems have been installed worldwide.<sup>2,8</sup> In addition to a lack of ionizing radiation which makes PET/MR very appealing for application in the paediatric population, MR offers superior soft tissue contrast compared to CT even without the use of contrast agents, particularly in tissues such as in cartilage, and bone marrow.

MR can also provide measurement of other factors that can characterize disease and their patient-specific biological properties, including blood vessels generated by a tumour, perfusion properties through dynamic contrast enhancement imaging and<sup>9</sup> cellular membrane integrity using diffusion weighted imaging.<sup>10</sup> Real-time image acquisition enables temporal co-registration of dynamic PET data acquisition and anatomical/functional MR data, providing a range of functional information, e.g. perfusion (micro vessel density, vessel leakage, etc.), diffusion (cell density, microstructure, etc.), and metabolism (cell death, proliferation, etc.)<sup>11</sup> to study the complex pathogenesis in infectious and inflammatory disorders.

\*Department of Biomedical Sciences, Humanitas University, Pieve Emanuele, Milan, Italy.

†Vascular Surgery Unit Department of Translational Research and Advanced Technologies in Medicine, University of Pisa, Pisa, Italy.

‡University of Groningen, University Medical Center Groningen, Medical Imaging Center, Groningen, The Netherlands.

§University of Twente, Faculty of Science and Technology, Biomedical Photonic Imaging, Enschede, The Netherlands.

||Regional Center of Nuclear Medicine, Department of Translational Research and Advanced Technologies in Medicine, University of Pisa, Pisa, Italy.

Address reprint requests to Paola Anna Erba, MD, PhD, Regional Center of Nuclear Medicine, University of Pisa, Via Roma 55, I-56125 Pisa, Italy. E-mail: p.erba@med.unipi.it

In this review, we summarize PET imaging of molecular processes in inflammatory and infectious diseases and outline the potential of PET/MR for these applications. A background to the main radiopharmaceuticals and some technical considerations also are included.

## Focus on Radiopharmaceuticals: Old and New Probes

Radiopharmaceuticals used in inflammation and infection imaging have been developed to target specific phase of the pathophysiology of each process. Therefore, knowledge of the specific pathophysiology pathways will facilitate an understanding of their applications as well as their advantages and limitations.

### PET Radiopharmaceuticals

Commercially available PET tracers have been used for imaging infection and inflammation. The two most widely applied radiotracers for infection and inflammation imaging are  $^{18}\text{F}$ -fluorodeoxyglucose ( $^{18}\text{F}$ FDG) and  $^{18}\text{F}$ -sodium fluoride ( $^{18}\text{F}$ NaF).  $^{18}\text{F}$ FDG PET is a widely used marker for glucose metabolism and is sensitive to areas of acute phase cellular response (neutrophils or PMNs),<sup>12</sup> but it's not limited to these cells subtypes, as monocyte-macrophages,<sup>13</sup> and CD4<sup>+</sup> T-lymphocytes<sup>14</sup> also are  $^{18}\text{F}$ FDG-avid. The molecular mechanism of  $^{18}\text{F}$ FDG uptake into cells relies on the presence of membrane glucose transporters, GLUT. Once internalized into the cells,  $^{18}\text{F}$ FDG is phosphorylated by hexokinase under kinetics similar to those of glucose. However, after the chemistry of the FDG prevents any further the metabolism or catabolism of the phosphorylated  $^{18}\text{F}$ FDG, which remains effectively trapped in the cell cytoplasm. Due to the variety of conditions that present high glucose metabolism and, consequent high  $^{18}\text{F}$ FDG uptake the differential diagnosis may be difficult and false-positive results should be always considered.

$^{18}\text{F}$ NaF is a long recognized bone-seeking agent that is able to probe bony remodelling.  $^{18}\text{F}$ NaF was first recognized as a bone-seeking agent in 1962<sup>15</sup> and approved for PET imaging by the United States Food and Drug Administration (FDA) in 1972. The mechanism of skeletal uptake of  $^{18}\text{F}$ NaF is based on ion exchange.<sup>16</sup> Bone tissue is continuously renewing itself through remodelling at the bone surface.  $^{18}\text{F}$  ions exchange with hydroxyl ions on the surface of the hydroxyapatite to form fluoroapatite.<sup>17</sup> This exchange occurs at a rapid rate; however, the actual incorporation of  $^{18}\text{F}$  ions into the crystalline matrix of bone may take days or weeks. Uptake of  $^{18}\text{F}$ NaF is a function of osseous blood flow and bone remodelling.  $^{18}\text{F}$ NaF uptake on PET images are interpreted as processes that increase exposure of the surface of bone and provide a higher availability of binding sites, such as osteolytic and osteoblastic processes.<sup>18</sup>  $^{18}\text{F}$ -sodium fluoride has been also used to identify areas of microcalcification in atherosclerotic plaque *in vivo*. Fluoride was shown to colocalize closely and preferentially bind to pathological

mineralization, and the increased surface area of microcalcification relative to macrocalcification resulted in increased tracer uptake.<sup>19</sup>  $^{18}\text{F}$ NaF uptake may occur at sites of macrocalcification, but distinct areas of  $^{18}\text{F}$ NaF uptake and macrocalcification occurring in isolation demonstrated that  $^{18}\text{F}$ NaF uptake reflects the active mineralization process in microcalcification rather than simply the burden of macrocalcification.<sup>20</sup> Plaque imaging is very promising and challenging application of PET/MR systems for the potential of identifying characteristics for the vulnerability of a plaque such as degree of stenosis, presence of thin cap with a large lipid core, endothelial denudation with superficial platelet aggregation, fissured/injured plaque and active inflammation.<sup>21,22</sup> In addition to  $^{18}\text{F}$ FDG and  $^{18}\text{F}$ NaF there are several other potential radiopharmaceuticals for the identification of plaque inflammation/vulnerability such as those targeting macrophage-driven inflammation (somatostatin receptor analogues,  $^{18}\text{F}$ -fluoromethylcholine/ $^{11}\text{C}$ -choline,  $^{68}\text{Ga}$ -pentixafor,  $^{11}\text{C}$ -PK11195) and inflammation and neovascularization (integrin  $\alpha_v\beta_3$ ).<sup>23,24</sup>

While radiolabelled granulocytes (WBC, Fig. 1) are a common clinical practice with SPECT applications, tracking WBC *in vivo* with PET using the positron emitting in still in the research phase. The short physical half-life of  $^{18}\text{F}$ , which has been used in the very first studies, is not suitable for late time imaging acquisition. In addition, non-specific uptake was observed when  $^{18}\text{F}$ FDG is used to label activated WBC mainly as a consequence of high efflux rate of  $^{18}\text{F}$ FDG shortly after the radiolabelling.<sup>25</sup> Different approaches have been developed for tracking radiolabelled leukocytes *in vivo* with PET using longer half-life isotopes such as copper-64 ( $^{64}\text{Cu}$ ,  $t_{1/2} = 12.7$  h) and zirconium-89 ( $^{89}\text{Zr}$ ,  $t_{1/2} = 78.4$  h). Cationic  $^{64}\text{Cu}^{2+}$  requires a chelate to transport it into cells;  $^{64}\text{Cu}$ -pyruvaldehyde-bis(N<sup>4</sup>-methylthiosemi-carbazone),  $^{64}\text{Cu}$ -polyethylenimine and  $^{64}\text{Cu}$ -loaded magnetic nanoparticles have been reported for WBC labelling.<sup>26-28</sup>  $^{64}\text{Cu}$ -PTSM proved to be superior to  $^{18}\text{F}$ FDG-labelled leukocytes with a higher and more reproducible labelling efficiency.<sup>29</sup>  $^{89}\text{Zr}$ -labelled nanoparticles have been used for *in vivo* macrophage imaging (dextran nanoparticles)<sup>30</sup> for *in vivo* cell trafficking with PET ( $^{89}\text{Zr}$ -oxinate)<sup>31</sup> and for radiolabelling mixed human leukocytes ( $^{89}\text{Zr}$ -loaded chitosan nanoparticles).<sup>32</sup> The highest labelling efficiency with  $^{89}\text{Zr}$  was observed with nanoparticles built from 190 to 310 kDa, and after a fast initial adhesion of the  $^{89}\text{Zr}$ -chitosan nanoparticles to the cell membrane a partial release was observed, leading to only a fraction of nanoparticles being internalised into the cell.<sup>32</sup>

Many other radiopharmaceuticals have been investigated for PET infection and inflammation imaging (Fig. 1) whereas for some of them only preliminary clinical data are currently available. For example, synovial angiogenesis in patients with rheumatoid arthritis (RA) was accomplished using  $^{68}\text{Ga}$ Gal-PRGD<sub>2</sub>.<sup>33</sup> The elevated agent uptake was detected in the sites of active inflammation, rich neovascularization, and physiological integrin receptor expression, while no tracer accumulation was detected in axillary lymph nodes with reactive hyperplasia and

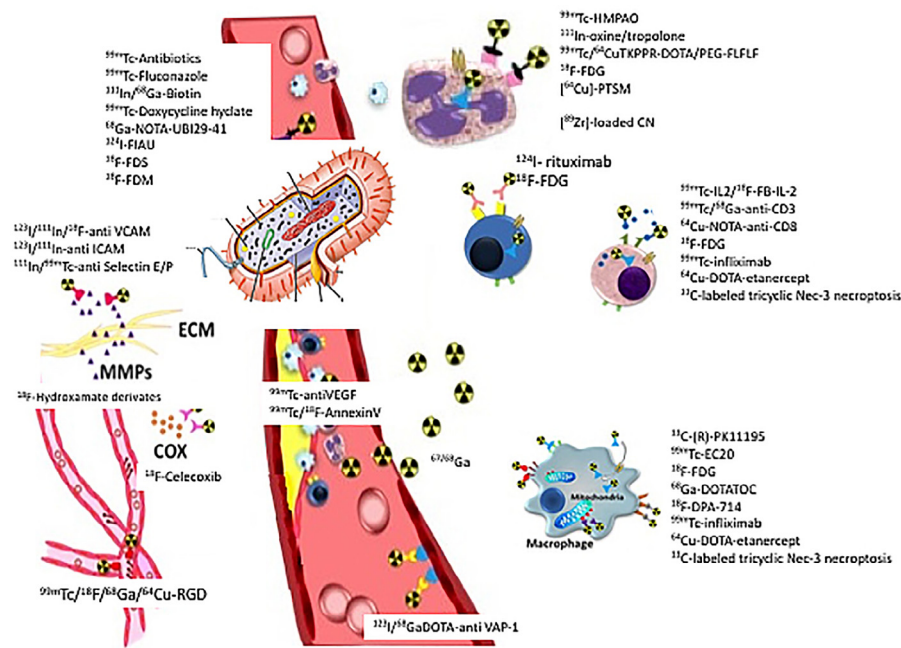


**Figure 1** Schematic representation of possible target of inflammation (Adapted from Theranostics 2013;3(7):448466).

strenuous skeletal muscles. [ $^{68}\text{Ga}$ ]Ga-pentixafor for detection and quantification of CXCR4 receptor density has been used for imaging chronic infection of the bone, such as osteitis/osteomyelitis of peripheral bone, osteomyelitis of the maxilla and infected endoprostheses.<sup>34</sup> [ $^{18}\text{F}$ ]fluoro-PEG-folate was investigated in patients with clinically active RA<sup>35</sup> providing the same positive results of the Tc-labelled folate moiety who showed accumulation in inflamed hand and foot joints of rheumatoid arthritis as compared to nonarthritis patient's hands and feet [ $^{36}$ ]. Iodine-124 1-(2'-deoxy-2'-fluoro- $\beta$ -D-arabinofuranosyl)-5-iodouracil ( $^{124}\text{I}$ -FIAU) is an example of a PET probe for bacterial infections, being a substrate for the native thymidine kinase from a wide variety of bacteria. A pilot study on musculoskeletal bacterial infections showed increased uptake of the radiopharmaceuticals in septic native joints, in prosthetic joints and in soft tissues.<sup>37</sup> However, further experience with [ $^{124}\text{I}$ ]FIAU PET/CT imaging argues against its potential as a robust imaging tool for PJI diagnosis. The specificity for bacterial infection was suboptimal. Metal artefacts in CT images resulted in pronounced PET signal localized to the prosthetic joint attributable to attenuation correction artefact, making the unequivocal detection of bacteria-specific uptake very challenging, particularly in cases where only a unilateral prosthesis was present.<sup>38</sup>

PK11195, a target agent that binds to the peripheral benzodiazepine receptor (PBR), a protein highly expressed in activated cells of the mononuclear phagocyte lineage, has been used for their clinical evaluation.<sup>39</sup> Indeed, since the early 1980s, [ $^{11}\text{C}$ ]PK11195 has been used for PET imaging of inflammatory diseases in the human brain on the basis of the low expression of PBRs in normal brain tissue and high expression in activated microglia, the resident phagocytes in brain tissue, during neuroinflammation.<sup>40</sup>

A very interesting novel approach based on the development of selective metabolic probes that are substrate for specific strains have recently renewed the interest in pathogen-specific imaging agents. In fact, while traditional approaches have been based on radiolabelling existing antibiotics (i.e. ciprofloxacin) or antimicrobial peptides (i.e. ubiquicidin)<sup>41</sup> designed to kill or disable bacteria at very minimal concentrations, thus potentially limiting their effectiveness as a radiotracer due to lack of signal amplification, researchers tested almost 1,000 radiolabelled small molecules as substrates for essential metabolic pathways in bacteria. Out of that, they identified 3 novel, nontoxic analogues of U.S. Food and Drug Administration (FDA)-approved compounds, PABA, D-mannitol and D-sorbitol and synthesized  $^3\text{H}$ -2-F-PABA,  $^3\text{H}$ -2-F-mannitol, and [ $^{18}\text{F}$ ]fluoro-deoxysorbitol ([ $^{18}\text{F}$ ]FDS).<sup>42</sup> *In vitro* and *in vivo* studies demonstrated that [ $^{18}\text{F}$ ]FDS avidly accumulates in *Enterobacteriaceae* infection foci, with little uptake in mammalian cells, sterile inflammation foci, or infection due to other bacteria species.<sup>43</sup> [ $^{18}\text{F}$ ]FDS holds tremendous potential for identifying and monitoring known or suspected infection caused by *Enterobacteriaceae*. In the first biodistribution study in healthy human volunteers,<sup>44</sup> after [ $^{18}\text{F}$ ]FDS administration, radioactivity was initially visualized in the vascular compartment and then rapidly distributed to the liver and kidneys. The radiotracer was mainly excreted through the urinary system. Radioactivity could be visualized in the urinary bladder as early as 5 min after [ $^{18}\text{F}$ ]FDS injection was eliminated through the kidneys mainly within 3 hrs. A small portion of the radiotracer was cleared into the gut through the hepatobiliary system. Segmental accumulation of [ $^{18}\text{F}$ ]FDS was observed in the small intestine. The gut radioactivity gradually moved towards the terminal ileum and finally into the ascending colon by the end of acquisition. The liver, spleen, and breasts demonstrated moderate

uptake, while the brain, lungs, thyroid, bone marrow, adrenal glands, and pancreas revealed only mild uptake.

## Bimodal Imaging Agent

Nowadays, even though there are many radiopharmaceuticals and contrast media available there is not the possibility of using a single probe for the simultaneous acquisition of PET/MRI. Therefore, the only way to exploit this interesting possibility is the administration of a cocktail of tracers (i.e. [ $^{18}\text{F}$ ]FDG for PET and Gd-DTPA for MRI at the same time). The basic idea of having a bimodal imaging agent is that by having two imaging reporters, the properties of both modalities can be synergistically combined. However, the obvious limitation is the different sensitivities of the two imaging techniques. In fact, whereas nuclear medicine techniques (i.e. PET and SPECT) have very high sensitivities (i.e. nanomolar or lower concentrations of imaging agent required), MRI has very low sensitivity (i.e. millimolar concentrations required). This enormous difference makes the addition of MRI reporters to radiotracers unrealistic. On the other hand, the addition of radionuclides to a MRI contrast agent is feasible. In this case, the different concentrations necessary for detecting both imaging signals require radiolabelling with very low specific activities. Adding a radionuclide to a MR contrast agent results in several advantages such as improved detection of low-contrast agent areas, as a consequence of the high sensitivity, and a better signal-to-noise ratio. In addition, the radionuclide signal of bimodal agents would allow more accurate and sensitive measurements of the biodistribution of the MR contrast agents, providing methods for the attenuation correction comparable to that which is performed with PET/CT scanners today. Using a bimodal PET/MR probe, it has proven suitable to use the PET for estimating the overall concentration of an agent and the MR signal to determine its molar relaxivity, giving an accurate estimation of the specific biochemical and physiologic target. In this perspective, efforts have been made to develop multimodal probes for PET/MR. Most of them are based on the bioconjugation of a tracer to a carrier, inducing the chemical modification of existing molecules or entrapping the diagnostic compound using not completely biocompatible materials. Examples of these dual probes include arginine-glycine-aspartic (RGD) conjugated to iron oxide nanoparticles,<sup>45</sup>  $^{124}\text{I}$  serum albumin conjugated with Mn-doped  $\text{Fe}_2\text{O}_3$ ,<sup>46</sup>  $^{64}\text{Cu}$  and Gd to evaluate fibrin imaging effect,<sup>47</sup>  $^{64}\text{Cu}$  associated with doxorubicin conjugated with SPIONs,<sup>48</sup> [ $^{18}\text{F}$ ]FDG adsorbed on core shell nanoparticles encapsulated with DTPA-Gd<sup>49</sup> and many others. As reviewed by Lahooti et al., the best targeting results are generally obtained with peptides or engineered mAb (with lower molecular weights) with an approximate hydrodynamic size of 40 nm, PEGylated radiolabelled with  $^{64}\text{Cu}$  or  $^{68}\text{Ga}$ . However, there are some exceptions and some good results have also been obtained with nanoprobes with a different composition.<sup>50</sup> At this stage, *in vitro* research has demonstrated the nanovector ability to improve the relaxometric properties and preserve the radioactivity without any chemical modification of the

molecules. Future developments will clarify their stability and biodistribution profile.

## Central Nervous System

PET is a noninvasive imaging procedure with a wide range of clinical and research applications in the evaluation of the pathophysiology of brain disorders, such as neurodegenerative diseases, infection, epilepsy, psychiatric disorders, and brain tumors, as well as in the study of neurophysiology of the normal brain. PET is referred to as a functional or molecular imaging tool that enables the study of biologic function in both health and disease, while MR provides morphologic information and can also evaluate some brain functions such as tissue perfusion and brain activation after performing a task, and connectivity.<sup>51</sup> Acquiring both PET and MR in a single session on a hybrid system is feasible, minimizing patient discomfort while maximizing clinical information, however some MRI attenuation correction-related PET errors may occur in neurodegenerative disease quantification.<sup>52</sup>

Although PET/MR potentially has great clinical utility in the evaluation of **encephalitis** and **brain infection**, few data are currently available, related to the relatively low incidence of these conditions and the relative scarce diffusion of the PET/MRI system. Case reports on voltage-gated potassium channel antibody-associated limbic encephalitis, neurocysticercosis, necrotizing granulomatous inflammation and neurosarcoidosis, have been reported, highlighting the value of PET/MR in the diagnostic and treatment monitoring setting.<sup>53-56</sup> Figure 2 shows an example of necrotizing granulomatous inflammation detected by  $^{68}\text{Ga}$ -DOTATATE PET/MR.<sup>55</sup> **Multiple sclerosis** (MS) is characterized by chronic inflammatory demyelination. PET/MR helps to obtain more specific information on the pathological mechanism of the disease. Translocator protein (TSPO)-targeted PET imaging has the ability to quantify neuroinflammation, to monitor disease progression, to predict prognosis, and to evaluate effects of treatment in MS.<sup>7,57</sup> [ $^{18}\text{F}$ ]FDG and [ $^{18}\text{F}$ ]fluoromethylcholine PET/MR have been used to assess the metabolic features of different variants of MS.<sup>58</sup>  $^{11}\text{C}$ -PIB, a PET tracer, originally developed for amyloid imaging, has been recently repropose to quantify demyelination and remyelination in MS. The use of myelin PET imaging, is limited due to its low resolution that deteriorates the quantification accuracy of white matter lesions. A multimodal partial volume correction approach by using PET/MR, allowing a better signal characterization of  $^{11}\text{C}$ -PIB uptake in lesions in both phantom and patients, has been recently proposed.<sup>59</sup> Immune and inflammatory mechanisms may play a fundamental role in the development of some forms of epilepsy.<sup>60</sup> Several lines of evidence support this assumption like the activation of the immune system in some patients with seizure disorders or the high incidence of seizures in some forms of autoimmune encephalitis. It has also been reported that various injuries lead to microglial activation, including status epilepticus in rats.<sup>61</sup> A hallmark in the neuropathology of temporal lobe epilepsy is brain

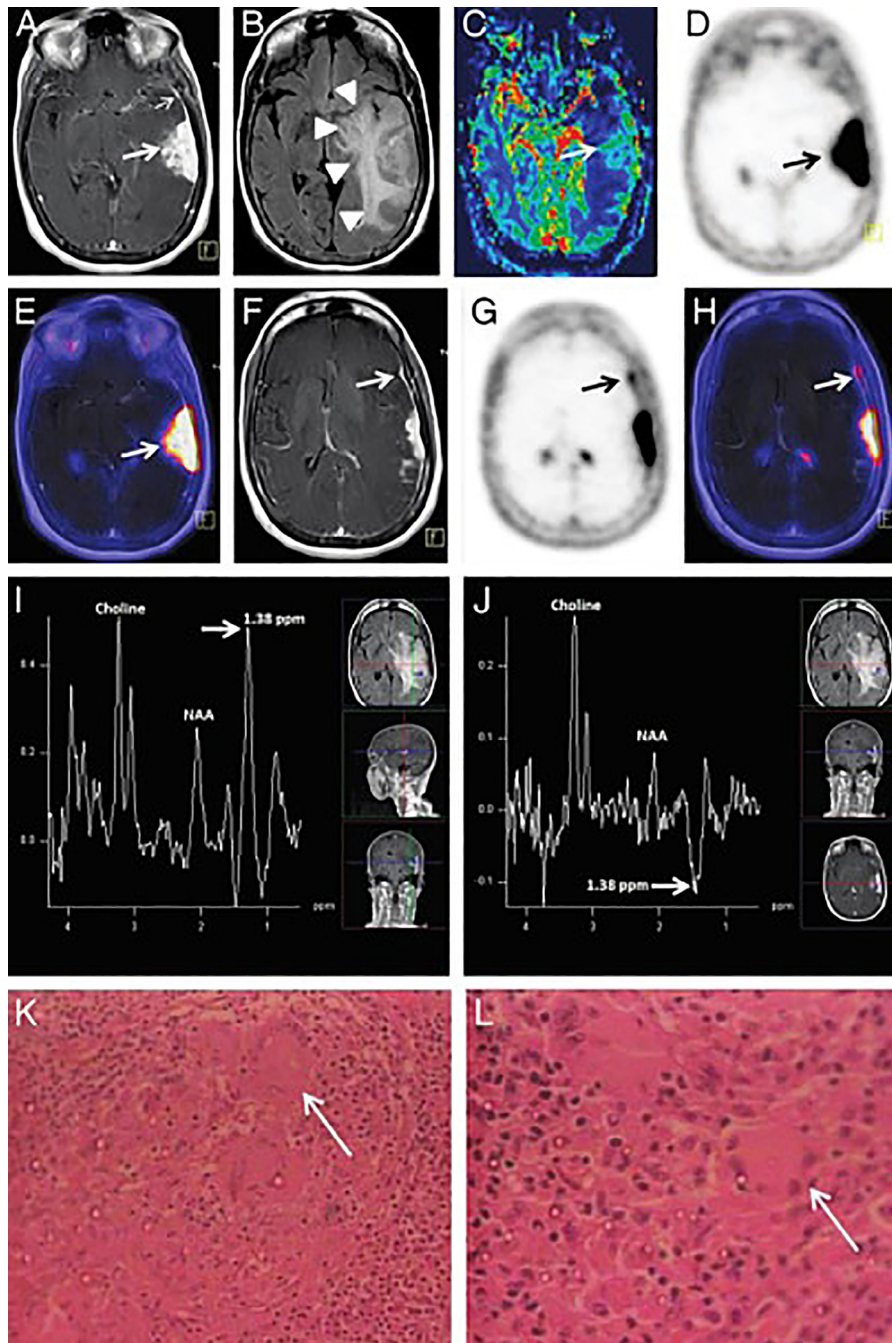


**Figure 2** Example of necrotizing granulomatous inflammation detected by  $^{68}\text{Ga}$ -DOTATATE PET/MRI. Contrast-enhanced axial T1 weighted MRI (T1W) images show an enhancing extra-axial, dural-based, space-occupying lesion in the left temporal region (arrow in A) with enhancement of the dura tail (small arrow in A) and associated white matter edema (arrowheads in B). MRI perfusion relative cerebral blood volume map shows increased regional perfusion (arrow in C). PET and PET/MRI images show  $^{68}\text{Ga}$  DOTATATE uptake in the enhancing lesion (arrows in D and E). Post-contrast T1W images reveal a subcentimeter-enhancing satellite lesion anteriorly (arrow in F) characterized by  $^{68}\text{Ga}$  DOTATATE uptake (arrow in G and H). Proton magnetic resonance spectroscopy identifies a lactate peak (arrow in I and J). Histopathologic examination of the specimen revealed well-formed noncaseating epithelioid granulomas (arrow in K and L). From Taneja S, Jena A, Kaul S, Jha A, Sogani SK. Somatostatin receptor-positive granulomatous inflammation mimicking as meningioma on simultaneous PET/MRI. *Clin Nucl Med*. 2015;40(1):e71-2. *Reprint permission requested*

inflammation which has been suggested as both a biomarker and a new mechanistic target for treatments. Non-invasive imaging of microglia activation biomarkers could be a relevant tool for detection, and especially for monitoring disease progression, therefore of great support to the evaluation of novel therapies<sup>62</sup> especially for epileptogenesis. Recently, inflammation has been demonstrated to be involved in neurodegenerative diseases. Immune cells, such as microglia and astrocytes, mediate the release of pro- and anti-inflammatory molecules. Their over- and underexpression, respectively, may result in neuroinflammation and thus disease onset and progression.<sup>63-66</sup> *In vivo*, microglial activation can be detected using PET ligands for the TSPO<sup>67,68</sup> and the reversible antagonist at TSPO [<sup>11</sup>C]-(*R*)-PK11195 is often used for studying diseases that involve microglial activation or the recruitment of macrophages as in multiple sclerosis,<sup>69</sup> stroke,<sup>70</sup> Alzheimer disease,<sup>71</sup> traumatic brain injury.<sup>72</sup>

Future investigations are foreseen to elucidate central nervous system diseases, taking advantage of new specific PET tracers targeting neuroinflammation and MRI advancement. The combination of the information provided by the two techniques may advance the knowledge and hopefully, contribute to the development of new therapeutic targets.

## Bone & Soft Tissue Infection

Imaging plays a major role in the diagnosis and management of musculoskeletal disease. MRI is able to provide multiple different structural and functional contrasts in soft tissue that are unavailable with any other imaging modality. In the clinical setting, MRI is the primary imaging system used to diagnose injuries in soft tissues such as intervertebral disc injuries; tears in the menisci, ligaments and tendons; as well as occult bone injuries. In addition, MRI is also widely used to study pathogenesis of many musculoskeletal disorders using advanced MRI techniques that provide unique functional information.<sup>73,74</sup> T2 and T1 rho relaxometry as well as magnetization transfer techniques provide information about cartilage biochemistry and have been shown to have significant prognostic value.<sup>75,76</sup> Further, arterial spin labelling<sup>77</sup> and chemical exchange saturation transfer<sup>78,79</sup> techniques are able to assess muscle perfusion and energetics, respectively. Although MRI is not typically associated with bone imaging, tissue diffusion<sup>80</sup> and ultra-short echo time<sup>81,82</sup> methods are able to provide important information about bone strength and fracture risk. Because MRI can offer novel functional contrasts, its combination with PET offers powerful observations of distinct physiological processes occurring in bone and cartilage at the same time.

Both [<sup>18</sup>F]FDG and [<sup>18</sup>F]NaF are very commonly used for PET imaging of musculoskeletal disorders.<sup>83</sup> As already discussed there are several interesting radiopharmaceuticals that are currently in the research setting and that hold promised in this specific field.<sup>33-35</sup> The introduction of PET/MR imaging adds a major dimension to research and clinical applications of PET in a variety of musculoskeletal disorders including

infection, diabetic foot, painful arthroplasty, metabolic bone marrow/bone disease, back pain, nonmalignant bone marrow disorders, and arthritis.

**Osteoarthritis** (OA) is a chronic, degenerative disease of the joint. Its pathogenesis is poorly understood. Inflammatory processes have been cited as a possible mechanism of OA tissue degeneration.<sup>84</sup> [<sup>18</sup>F]NaF-PET/MRI systems allow for comprehensive imaging of the whole joint in OA, including soft tissues and bone, offering the opportunity to simultaneously assess the role of metabolic activity, and relate it to qualitative MRI metrics of bone pathologies.<sup>84</sup> One of the biggest benefits of hybrid PET/MR imaging of OA is the ability to simultaneously evaluate molecular and morphologic spatial relationships across multiple tissues (metabolic bony activity in subchondral bone pathology and cartilage morphology) and by using [<sup>18</sup>F]FDG, it may also provide complementary information linking changes in the soft tissues with bone remodeling and inflammation.

**Ankylosing spondylitis** (AS) is a fairly common autoimmune-mediated chronic inflammatory disease that predominantly affects the spine and the sacroiliac joints. The simultaneous acquisition of high-resolution anatomical and functional MR images and metabolic information by [<sup>18</sup>F]NaF-PET provides new insights into the link between inflammatory cascades, local metabolic changes, and the development of structural manifest inflammation in AS.<sup>85</sup> **Rheumatoid arthritis** is an autoimmune disease, associated with systemic and chronic inflammation of the joints, resulting in synovitis and pannus formation. For many years, the evaluation of RA has been restricted to conventional radiography, even though this technique lacks sensitivity for detecting the inflammatory process that occurs in the initial stages. Additionally, the introduction of biological treatments claims for other imaging modalities able to achieve an early diagnosis and an adequate follow-up.<sup>86</sup> Conventional nuclear medicine provides a great contribution to RA imaging. The introduction of [<sup>18</sup>F]FDG-PET technology, sensitive to inflammatory changes within the synovial tissue, presenting some advantages than conventional imaging such as a higher spatial resolution and quantification, increases the use of molecular imaging in RA. In particular, [<sup>18</sup>F]FDG-PET/MR provides metabolic information which has the potential to assess different aspects of arthritis such as bony disintegration and inflammatory activity, together with the precise anatomical and morphological data and the excellent soft tissue contrast, maximizes the strengths of both imaging approaches in RA imaging<sup>87</sup> and treatment monitoring.<sup>88</sup> In addition to [<sup>18</sup>F]FDG, other tracers may be used to image RA. The relationship between synovial hypoxia and synovial inflammation has been evaluated. Hypoxia-inducible factors play a major role in RA disease progression, acting as key regulators of inflammation.<sup>89</sup> Preclinical data have shown that noninvasive imaging of inflammation-induced hypoxia in arthritic joint inflammation with PET/MR and hypoxia-specific radiotracer (<sup>18</sup>F-fluoromisonidazole and <sup>18</sup>F-fluoroazomycin-araboside) might be a promising clinical tool for uncovering affected, but clinically silent, joints at an early stage.<sup>90</sup> The diagnosis of **spondylodiscitis**

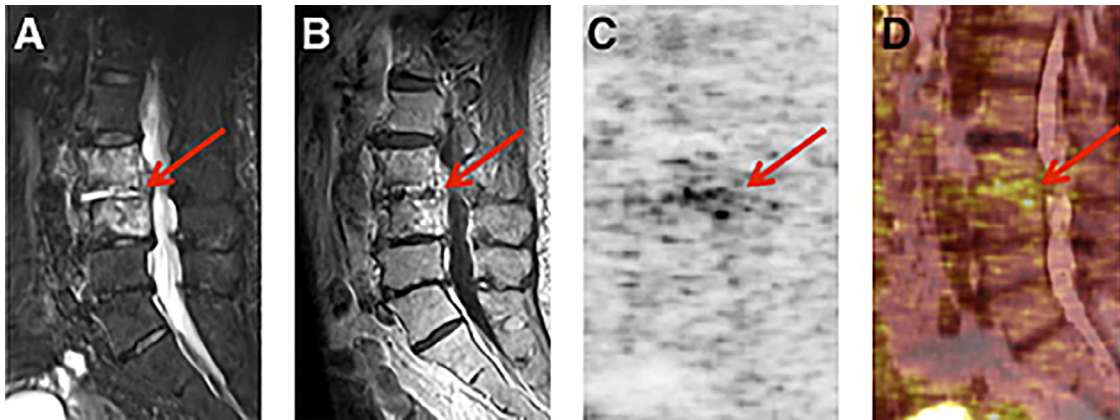


**Figure 3** Simultaneous [ $^{18}\text{F}$ ]FDG PET/MRI in 71-y-old female patient with final diagnosis of spondylodiscitis. MRI alone was inconclusive. (A) TIRM with typical hyperintense signal alterations at intervertebral disk level L4–L5 (arrow). (B) Moderate postcontrast signal (arrow) on T1-weighted MRI. (C and D) [ $^{18}\text{F}$ ]FDG PET (C) and combined [ $^{18}\text{F}$ ]FDG PET/MRI (D) show focally elevated uptake in affected disk (arrow;  $\text{SUV}_{\text{max}}$ , 8.14;  $\text{SUV}_{\text{mean}}$ , 3.99) as sign of active inflammation. This research was originally published in *JNM*. Simultaneous [ $^{18}\text{F}$ ]FDG PET/MRI in 71-y-old female patient with final diagnosis of spondylodiscitis. Jeanette Fahnert et al. *J Nucl Med* 2016;57:1396-1401 © by the Society of Nuclear Medicine and Molecular Imaging, Inc.

(SD) is often challenging. MRI is sensitive (up to 96%) but lacks specificity in the presence of fractures or spinal implants, and distinction from erosive osteochondritis is often difficult. [ $^{18}\text{F}$ ]FDG-PET/MR improves diagnostic certainty for the detection of SD (sensitivity = 100% and specificity = 88%) compared to MRI assessment, especially in patients with inconclusive clinical or MRI findings.<sup>91</sup> Figure 3 shows an example of [ $^{18}\text{F}$ ]FDG PET/MRI in a patient with SD.

In **diabetic foot infections** imaging has a pivotal role in clinical decision making since it helps to diagnose soft tissue infection and osteomyelitis, to differentiate Charcot arthropathy from osteomyelitis, and to evaluate ischemia/atherogenesis component in some cases.<sup>92</sup> PET/MR could improve accuracy in detecting soft tissue lesions in osteomyelitis [65]. Additionally, it would be useful to quantify PET detectable functional changes and spectroscopy measurable metabolites simultaneously in diabetic neuropathy.<sup>93</sup> Because of the

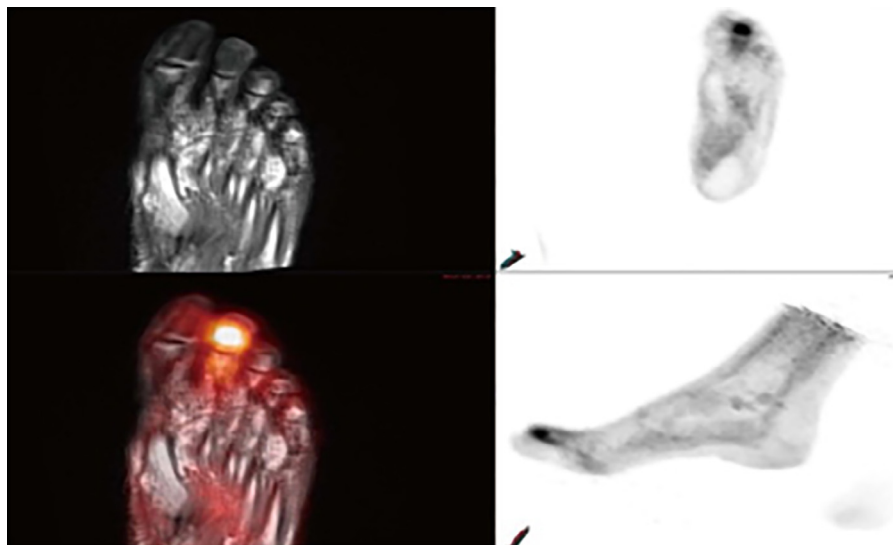


**Figure 4** A 71-year-old male with poorly controlled diabetes and end-stage renal disease presents with worsening right foot pain. Bone scan revealed diffuse radiotracer uptake within the right foot without focal abnormality. MRI of the right foot demonstrates diffuse abnormal T1 and T2 signal within the right foot digits. Multiplanar PET/MRI images reveal focal [ $^{18}\text{F}$ ]FDG uptake within the distal right second digit with corresponding heterogeneous T1 hypointense, T2 hyperintense signal compatible with osteomyelitis. PET: Positron emission tomography; MRI: Magnetic resonance imaging; FDG: [ $^{18}\text{F}$ ]fluorodeoxyglucose. From Chaudhry AA, Gul M, Gould E, Teng M, Baker K, Matthews R. Utility of positron emission tomography-magnetic resonance imaging in musculoskeletal imaging. *World J Radiol* 2016; 8(3): 268-274. Reprint Permission Requested



limited availability of this hybrid scanner as of today, PET/MR cannot be considered an established modality for clinical practice in diabetic foot [65]. Figure 4 shows an example of PET/MR in Charcot disease.<sup>94</sup> In patients with prostheses, PET/MR has been used for technical purpose (i.e. artefacts due to metal implants and images reconstruction) rather than clinical ones (i.e. loosening/infection).<sup>85</sup>

## Cardiovascular System

Specific requirements have to be fulfilled when PET/MR is used to image the cardiovascular system. Therefore before reviewing the most important applications of PET/MR in cardiovascular infection and inflammation, we will discuss some of the details of these requirements, including proper patient preparation and motion correction algorithms.

### Patient Preparation

[<sup>18</sup>F]FDG is often used for the evaluation of inflammatory processes since these conditions are characterized by increased glucose uptake by macrophages and other inflammatory cells. Therefore, suppression of physiological myocardial [<sup>18</sup>F]FDG uptake is mandatory and usually obtained with dietary restriction.<sup>95,96</sup> A recent study showed that a high fat, low carbohydrate diet without fasting is successful in suppressing [<sup>18</sup>F]FDG uptake in 84% of patients.<sup>97</sup> A recent procedural joint statement on myocardial [<sup>18</sup>F]FDG imaging in inflammation is available.<sup>98</sup> The main goal of adequate patient preparation imaging large vessel vasculitis (LVV) is to reduce physiologic tracer uptake in normal tissues (myocardium, skeletal muscle, urinary tract and brown adipose tissue) while maintaining uptake in diseased tissues and organs. Glucocorticoids (GC) may reduce vascular wall uptake of [<sup>18</sup>F]FDG: few data are available on the effect of GC withdrawal on [<sup>18</sup>F]FDG uptake. It is confirmed recently that the diagnostic accuracy of LVV with [<sup>18</sup>F]FDG PET remains for up to 3 days after initiation of GC, thereafter the uptake decreases significantly.<sup>99,100</sup> Therefore, there may be a diagnostic window of opportunity within 3 days of initiation of GC.

### Motion Correction Algorithms and Attenuation Correction

Cardiac and respiratory motion can degrade image quality leading to a reduced diagnostic accuracy of PET/MR scans. In particular, the presence of motion artefacts can negatively affect myocardial attenuation maps resulting into false positive perfusion defects. Therefore, motion correction is mandatory to obtain diagnostic images and to improve the co-registration between PET and MR images.<sup>101</sup> Motion compensation due to cardiac contraction is usually obtained synchronizing PET image acquisition to the ECG allowing the reconstruction of images in the same, near

“motion-free”, phase of the cardiac cycle. A similar approach can be applied also for respiratory motion correction combining data obtained at analogous respiratory positions from multiple breathing cycles.<sup>102</sup> While these gating approaches have been widely used in several static PET acquisitions, they are not so efficient for four-dimensional (dynamic) PET studies due to the insufficient number of detected counts available for each reconstruction.<sup>102</sup> In order to obviate this problem, using more sophisticated approaches, motion information can be derived directly from PET data<sup>103,104</sup> for first from high-resolution anatomical MR images and then applied to PET images.<sup>105</sup>

Traditionally, cardiovascular imaging has been performed in PET-only and PET/CT systems by relying on attenuation correction (AC) maps obtained from a rotating transmission source or CT measurement, respectively. In hybrid PET/MR systems, these options are not available and alternative solutions have to be found. In general, segmented MR-based AC (DIXON MR-AC) maps are currently chosen as AC method-of-choice for integrated PET/MR imaging. Transformation from MR-images into AC maps are based on segmentation algorithms, which segment the images into four tissue types, with each tissue classification assigned to a vendor-specific attenuation (ATN) value.<sup>106</sup> In general, myocardial FDG imaging obtained from MR-based attenuation corrected [<sup>18</sup>F]FDG PET is comparable to standard CT-based attenuation corrected FDG PET, suggesting interchangeability of both AC techniques.<sup>107</sup> In MRI, non-magnetic metals cause a signal void that exceeds the actual size of the object, which in turn might result in an underestimation of the attenuation. More importantly, however, these devices may interact with the radiofrequency and cause malfunction or sometimes heating of the leads of electronic heart devices. As a consequence, some patients cannot be examined using MR (and thus by PET/MRI).

### Cardiovascular Applications of PET/MR Imaging

Cardiac MR and cardiac [<sup>18</sup>F]FDG PET are both well-established techniques in the evaluation of inflammatory myocardial diseases. With a multi-parametric approach MR provides anatomical information regarding myocardial oedema (T2 sequences), focal or diffuse myocardial fibrosis (late gadolinium enhancement, LGE, and T1 mapping) and myocardial contractility. On the other hand, [<sup>18</sup>F]FDG PET imaging can assess the status of the disease allowing the functional evaluation of the extension and the degree of the inflammatory process. Despite this potential complementary role, the additional value of this hybrid approach over the use of each single modality alone, in terms of diagnosis and cardiovascular risk stratification, has still to be proven.

Heart involvement is an adverse prognostic factor in patients with **sarcoidosis** and it usually manifests as heart failure and new onset cardiac arrhythmia. Although accurate diagnosis of subclinical but active **cardiac sarcoidosis**

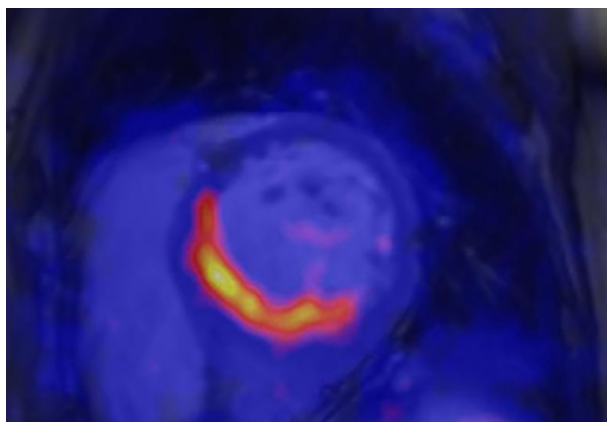


**Figure 5** Example of [ $^{18}\text{F}$ ]FDG PET/MR in a woman, 57 yrs old, with sarcoidosis. Images shows positive signal on MRI T1 and T2, and [ $^{18}\text{F}$ ]FDG uptake in the inferoseptal wall. Reduced LVEF and wall motion disturbances were present.

is the key to guide patient therapy and to prevent long-term complications, a gold standard imaging technique is lacking. Both cardiac MR and [ $^{18}\text{F}$ ]FDG PET imaging are currently used clinically for the diagnosis of cardiac sarcoidosis<sup>108-110</sup> with comparable diagnostic performance.<sup>111</sup> In this pre-simultaneous PET/MR imaging images are usually interpreted independently, losing the complementary information they provide. The feasibility of imaging cardiac sarcoidosis with hybrid PET/MR systems was initially described in a few case reports which showed accurate anatomical correlation between areas of fibrosis on MR delayed enhanced images and increased activity on PET imaging.<sup>112,113</sup> Recently, Dweck and colleagues demonstrated that the simultaneous acquisition of MR and PET images provides accurate localization of myocardial injury on late enhancement images and disease activity on PET allowing the differentiation of patients with active disease from patients with inactive disease. In addition, the combination of negative LGE but positive, diffuse [ $^{18}\text{F}$ ]FDG myocardial uptake on PET images allowed the identification of false positive findings due to incomplete myocardial suppression.<sup>114</sup> **Figure 5** shows an example of PET/MR in a patient with cardiac sarcoidosis. Besides early diagnosis, other potential applications of PET/MR could be the monitoring of disease response to therapy and the estimation of individual risk assessment.<sup>115</sup> A multimodality imaging approach may be necessary for instance for decision making about pacemaker or ICD.<sup>110</sup> MR is less specific for inflammation. However, they may help in the assessment of LV remodeling, left as well as right ventricular function, pulmonary artery hypertension and in the follow-up of end stage heart failure from cardiac sarcoidosis. Observational studies suggest an important role for [ $^{18}\text{F}$ ]FDG PET for monitoring efficacy of immunosuppressive therapy,<sup>116</sup> for accurate differentiation of residual myocardial inflammation from fibrosis.

Novel PET radiopharmaceuticals for imaging cardiac sarcoidosis are being investigated with the benefit of no

background uptake, such as somatostatin receptor based hybrid imaging.<sup>117,118</sup> The somatostatin receptor subtype 2 (SSTR2) is highly expressed in sarcoid granulomas and several  $^{68}\text{Ga}$ -labeled somatostatin analogues are able to image this.

Cardiac MR is considered the reference standard in the diagnosis of **myocarditis** in patients presenting with chest pain, raised troponin and normal coronary arteries.<sup>119,120</sup> Few case reports demonstrate good correlation between areas of epicardial fibrosis detected on LGE, oedema and hyperemia and [ $^{18}\text{F}$ ]FDG uptake on PET images (**Fig. 6**).<sup>121,122</sup> T2 mapping had the highest correlation rate with [ $^{18}\text{F}$ ]FDG uptake.<sup>121</sup> Besides confirming the diagnosis of myocarditis, PET/MR may have a role in improving the diagnostic accuracy of cardiac MR in the detection of chronic myocarditis.<sup>119</sup> In addition, PET/MR can provide additional information on inflammatory activity, which is critical for monitoring therapeutic response. Novel PET tracers for the evaluation of myocarditis are currently under investigation. In a rat model of autoimmune myocarditis,  $^{11}\text{C}$ -methionine PET imaging was able to detect foci of myocardial inflammation.<sup>123</sup> The advantage of using this tracer is that there is no need for dietary restriction since there is no physiological myocardial  $^{11}\text{C}$ -methionine uptake. The combined approach of [ $^{18}\text{F}$ ]FDG PET/MR may result in improved diagnosis. However, even though there is accumulating evidence for this approach, further studies are warranted.

**Large vessel vasculitis (LVV)** is defined as a disease affecting mainly large arteries, with two major variants, Takayasu arteritis (TA) and giant cell arteritis (GCA).<sup>124</sup> Vasculitis can be distributed locally in the branches of the internal and external carotid artery or the aorta and its main branches more central in the thorax. GCA and TA also show some overlap, regarding histopathology of arterial lesions reflecting shared pathways in tissue inflammation.<sup>125</sup> [ $^{18}\text{F}$ ]FDG PET and MRI solely can identify the presence of systemic LVV in patients with GCA and TA. Morphological imaging is represented mainly by MRI. Increased vessel wall thickness (usually with a diffuse circumferential pattern), associated with vessel wall edema on T2 and fat-suppressed sequences, and mural contrast enhancement on T1 sequences are early signs of vascular inflammation. Post-contrast T1 images are superior to T2 or fat-suppressed images to detect early large vessel inflammation. Moreover, MRI angiography (MRA) provides luminal information, such as arterial stenosis, occlusion and dilatation. In active LVV, there is increased [ $^{18}\text{F}$ ]FDG uptake by the vessel wall, typically with a smooth linear pattern, showing elevated uptake in inflammatory association cells, such as macrophages, monocytes and lymphocytes (chronic LV phase). To date, there is only study, which compared the diagnostic performance of [ $^{18}\text{F}$ ]FDG PET/MR and [ $^{18}\text{F}$ ]FDG PET/CT. Einspieler et al., studied a total of 16 [ $^{18}\text{F}$ ]FDG PET/MRI and 12 [ $^{18}\text{F}$ ]FDG PET/CT examinations were performed in 12 patients with LVV (**Fig. 7**).<sup>126</sup> MRI of the vessel wall by T1-weighted and T2-weighted sequences was used for anatomical localization of FDG uptake and identification of morphological changes associated with LVV. In addition,

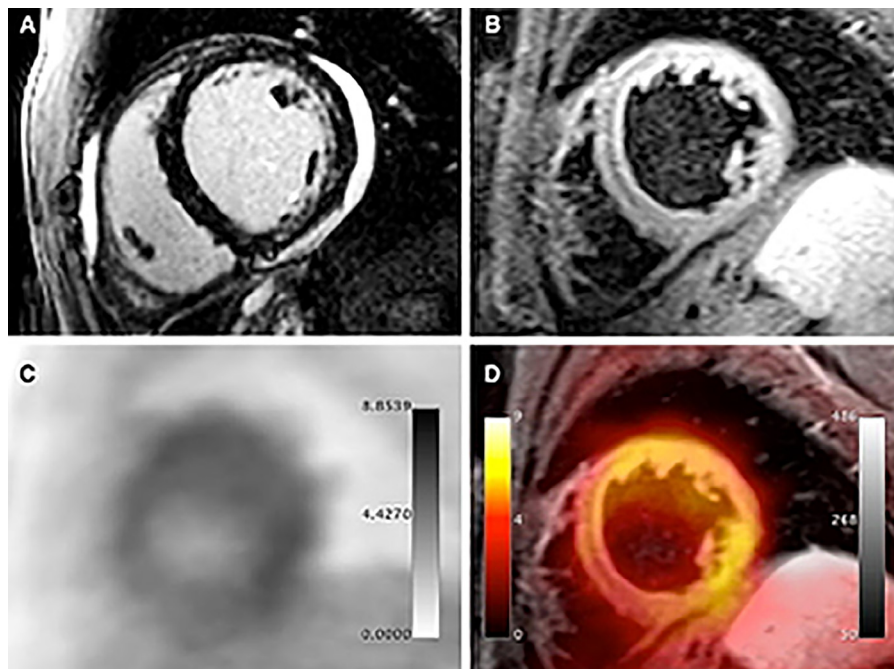


**Figure 6** [ $^{18}\text{F}$ ]FDG PET/MRI examination in a 32-year-old male presenting with dyspnoea, mild ventricular dysfunction (51% LFEV), and a history of recent systemic viral disease. Patchy intramyocardial late gadolinium enhancement in the lateral and inferior wall as well as pericardial effusion. B shows significantly increased T2 signal in the lateral wall representing myocardial oedema. C (PET) and D (fusion between T2-weighted MR image and PET) show diffusely increased [ $^{18}\text{F}$ ]FDG uptake in the lateral, anterolateral, and inferolateral wall. Histopathological assessment after endomyocardial biopsy showed acute myocarditis with lymphocytic infiltration and moderate myocyte apoptosis. The patient demonstrated elevated levels of C-reactive protein (4.1 mg/dl) as well as elevated myocardiocytolysis serum markers (Troponin-I: 0.42 ng/ml). PCR and immunohistochemical analysis did not detect specific infectious agents such as viruses, bacteria, or fungi. From Nensa F, Kloth J, Tezgah E, Poeppel TD, Heusch P, Goebel J, et al. Feasibility of FDG-PET in myocarditis: Comparison to CMR using integrated PET/MRI. *J Nucl Cardiol*. 2016. *Reprint permission requested*

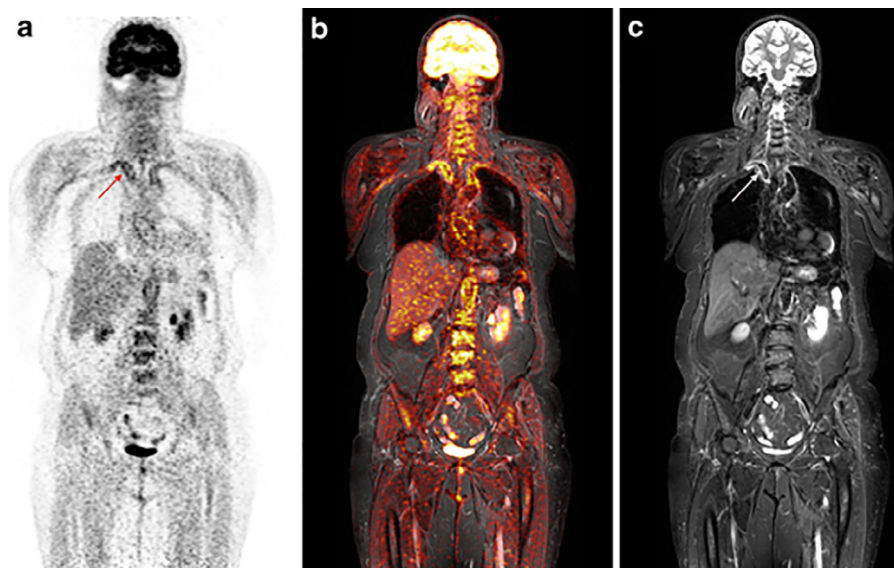


**Figure 7** Signal elevation (indicating oedema) and visual wall thickening of the right subclavian artery in the coronal T2w STIR (white arrow; c) with corresponding pathological [ $^{18}\text{F}$ ]FDG uptake in the coronal positron emission tomogram (red arrow; a), best seen on the fused PET/MRI images (b). Einspieler I, Thürmel K, Pyka T, Eiber M, Wolfram S, Moog P, et al. Imaging large vessel vasculitis with fully integrated PET/MRI: a pilot study. *Eur J Nucl Med Mol Imaging*. 2015;42(7):1012-24. *Reprint permission requested*

contrast-enhanced MRA was performed. The vascular FDG uptake in the vasculitis group was compared to a reference group of 16 patients using a four-point visual score.<sup>127</sup> Visual scores and quantitative parameters [maximum standardized uptake value (SUV<sub>max</sub>) and target to background ratio (TBR)] were compared between PET/MR and PET/CT. In this study the authors showed that adding the anatomical information provided by MR the number of vascular segments classified as vasculitic by PET imaging increased from 86 to 95.<sup>126</sup> Promising, still unexplored fields of application include endocarditis and vascular prosthesis inflammation where quantification of disease activity may have an additional value, in particular for therapy monitoring.

## Abdominal Diseases

PET/MR, enabling the simultaneous registration of dynamic and moving phenomena, is particularly important in the evaluation of the abdomen where the relative positions of organs may be altered due to peristaltic motion and bladder filling. Moreover, both PET and MRI images are acquired simultaneously under the same physiological conditions, which is particularly important in the evaluation of abdominal diseases.<sup>128</sup> Imaging plays a pivotal role in the diagnosis and management of inflammatory bowel disease (IBD).<sup>129</sup> In fact, monitoring subclinical inflammation is crucial, since it will affect the treatment strategy and disease outcome.<sup>130,131</sup> Although endoscopy is the gold standard for the evaluation of **inflammatory bowel diseases** (IBD), non-invasive imaging has been extensively used in this setting. Because of the lack of ionizing radiation, the bowel can be imaged by MR at multiple time points, providing a dynamic assessment of mural signal intensity and enhancement to assess both active and chronic inflammatory changes.<sup>129</sup> Many MR features (hyperintensity of the intestinal wall on diffusion-weighted imaging, rapid gadolinium enhancement, differentiation between the mucosa-submucosa complex and the muscularis propria, bowel wall thickening, parietal edema, and the presence of ulceration) have been reported to be associated to endoscopic findings in ulcerative colitis (UC).<sup>131</sup> MR performs better in moderate to severe UC than in mild cases<sup>132</sup> and its role in the differentiation of a quiescent lesion from an active lesion in UC is not defined.<sup>131</sup> Crohn's disease (CD). In quiescent Crohn's disease (CD) patients, the presence of restricted diffusion in the distal ileum is suggestive of an active inflammation. Therefore MR-DWI may serve as a clinical tool in the follow-up of these patients implying subclinical inflammatory flares.<sup>133</sup> More recently [<sup>18</sup>F]FDG PET/CT has been applied in IBD. PET has been reported to be sensitive tool for detecting intestinal inflammation (pooled sensitivity of 84%, specificity of 86% on per-bowel-segment analysis<sup>134</sup> [75]) however, its role in quiescent UC is not established yet.<sup>131</sup> Few promising results have been reported on the use of PET/MR in IBD evaluation. Particularly, [<sup>18</sup>F]FDG PET/MR was useful for identifying subclinical

inflammation in UC<sup>131</sup> and PET/MR enterography biomarkers (SUV<sub>max</sub>, signal intensity on T2-weighted images × SUV<sub>max</sub>, and apparent diffusion coefficient × SUV<sub>max</sub>) was successfully used to differentiate purely fibrotic strictures from mixed or inflammatory strictures in CD.<sup>135</sup> Additionally PET/MR-enterography has been reported to be highly accurate in the assessment of CD lesions including extra-luminal disease and distant localization before operation, thus contributing to clinical management of patients with small-bowel CD.<sup>136</sup> **Figure 8** presents an example of PET/MR in a patient with cecal inflammation.

Fully integrated [<sup>18</sup>F]FDG PET/MRI was also evaluated in **retroperitoneal fibrosis** showing better performance as compared to clinical and inflammatory parameters to assess disease activity as well as the ability to detect associated large-vessel vasculitis and aneurysms that may occur apart from the site of the retroperitoneal fibrosis.<sup>137</sup>

Recently, [<sup>18</sup>F]FDG PET/MRI has been used for the management of a parasitic disease, in a patient with *Echinococcus multilocularis*. Images show peri-lesional uptake in a hepatic lesion, opening the possibility to further systematic evaluation of the technique in the routine management of alveolar echinococcosis (**Fig. 9**).<sup>138</sup>

## Paediatric Population

Paediatric imaging has emerged as a key application of combined PET/MR, especially in the context of paediatric oncology.<sup>139</sup> Advantages of the technique in this special patient population include high imaging quality, significantly lower radiation exposure and a reduction in the total number of required imaging studies, which simplifies clinical workflows and reduced the number of necessary sedation in younger children. Specific imaging protocols for children and young adults are currently under investigational evaluation. Preliminary results show that a gadolinium-free cancer PET/MR staging of children and young adults provided superior tumor diagnosis and 74% reduction in effective dose compared to standard clinical imaging tests. In this series, PET/MR provided clinically important detail about the primary tumor and excellent detection of pulmonary nodules ≥5 mm.<sup>140</sup> The role of PET/MRI in non-oncologic imaging has not been this clearly defined in children yet despite numerous non-oncologic applications are conceivable such as in case of fever of unknown origin or inflammatory conditions (i.e. chronic inflammatory bowel disease, rheumatoid disorders or chronic infectious disease). **Figure 10** shows an example of PET/MR in a 17-year-old girl with acute lung inflammation in cystic fibrosis.

## Conclusions

PET/MR has gained momentum in the areas of oncology and neuroscience whereas research in the field of infection and inflammation are still very limited. Currently, PET/MR imaging

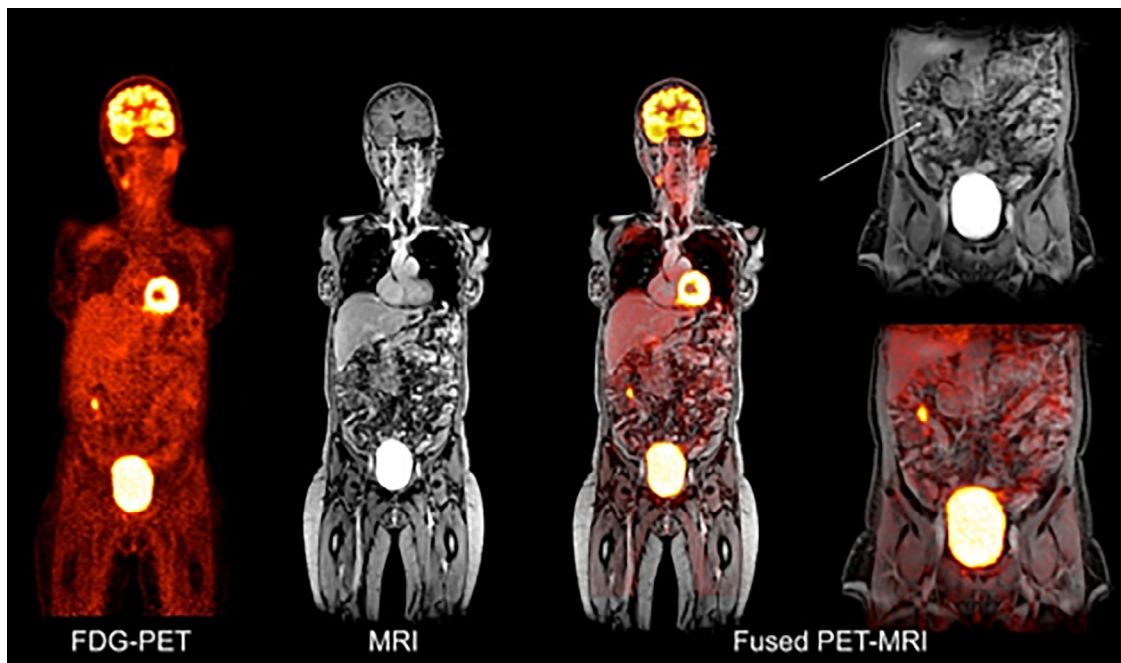


**Figure 8** PET/MRI of patient with cecal inflammation. Fused imaging demonstrates small area of active inflammatory changes in the cecum that would be difficult to diagnose on either  $[^{18}\text{F}]\text{FDG}$ -PET or MR imaging independently. From Rahul A. Sheth and Michael S. Gee (2012). *The Imaging of Inflammatory Bowel Disease: Current Concepts and Future Directions*, Inflammatory Bowel Disease, Dr. Imre Szabo (Ed.), InTech, DOI: 10.5772/53025. Available from: <https://www.intechopen.com/books/inflammatory-bowel-disease/the-imaging-of-inflammatory-bowel-disease-current-concepts-and-future-directions>

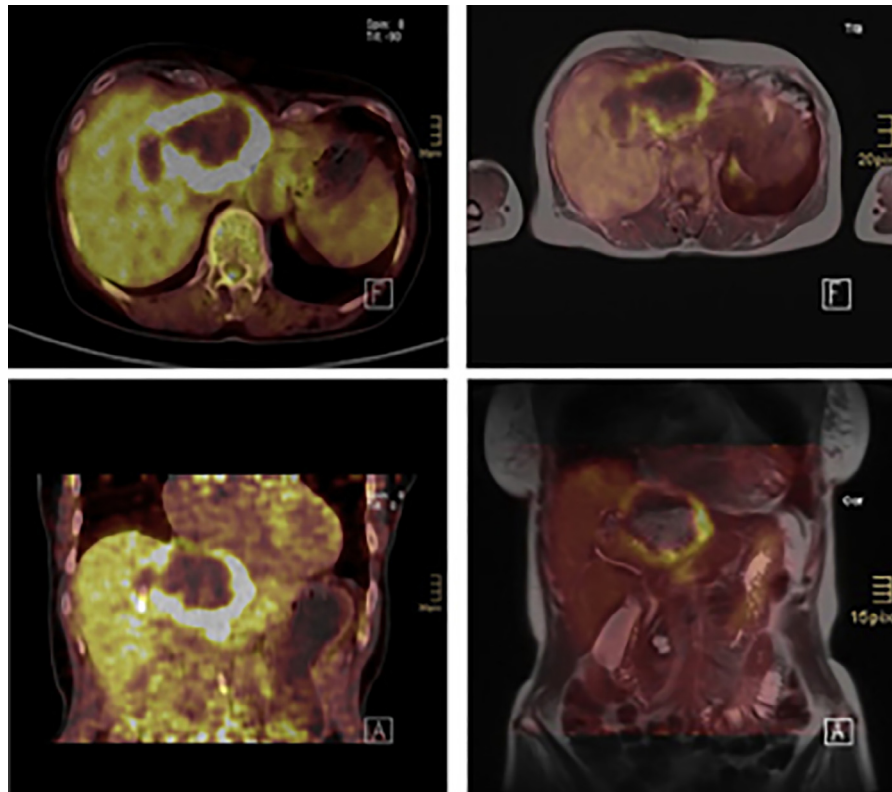


**Figure 9** Axial (upper row) and frontal (lower row) sections from  $[^{18}\text{F}]\text{FDG}$  PET/CT (left) and  $[^{18}\text{F}]\text{FDG}$  PET/MRI (right), showing strong peri-lesional uptake in a patient with a hepatic lesion caused by *Echinococcus multilocularis*—the fox tape worm. Felix Lötsch, Fredrik Waneck, Herbert Auer, Klaus Kaczirek, Georgios Karanikas, Michael Ramharter. From *FDG-PET/MRI in alveolar echinococcosis* *International Journal of Infectious Diseases* Volume 64, Pages 67-68 (November 2017) DOI: 10.1016/j.ijid.2017.09.006

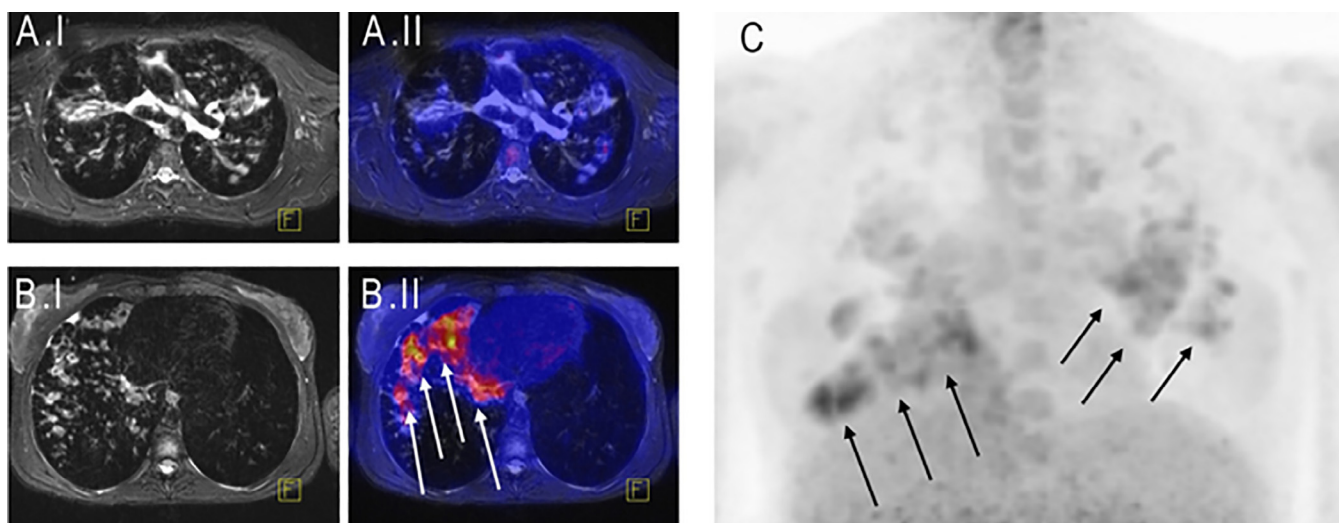


**Figure 10** 17-year-old girl with severe pulmonary manifestations of cystic fibrosis, referred to exclude an acute pulmonary infection before planned lung transplantation. MRI (transversal T2 w TSE sequence, A.I and B.I) shows inflammatory changes but cannot discriminate between chronic and acute inflammation. [ $^{18}\text{F}$ ]FDG-PET (A.II, B.II, C) shows active inflammation of the lower lobes. Gatidis S, Bender B, Reimold M, Schäfer JFEur J Radiol. 2017 Sep;94:A64-A70. doi: 10.1016/j.ejrad.2017.01.018. PET/MRI in children. Reprint permission requested

is likely the most strongly emerging research platform in imaging science, and over the next few years, it will show its potential for providing new options in clinical diagnosis. Preclinical studies have indicated several potential new radiopharmaceuticals that warrant clinical research in this specific field of investigation. In the near future, PET/MR imaging studies in infection and inflammation should be more and more focused on the whole integration of the multiparametric functional information offered by both modalities rather than limited to the use of the MR information as a mere anatomic landmark for the functional information from PET. Accordingly, clinical studies providing the value of PET and MR imaging through the synergy arising from their combination rather than the comparison of the results with other modalities as PET/CT in terms of sensitivity and specificity are foreseen. The complexities of MR physics, MR sequence optimization, artifacts, the functional aspects of MR imaging, and a huge volume of intricate anatomy will require specific education and training, thus representing the next challenge for the nuclear medicine community to unravel the full potential of this new technology and to make it entering into daily clinical practice.

## References

1. Ter-Pogossian MM, Phelps ME, Hoffman EJ, et al: A positron-emission transaxial tomograph for nuclear imaging (PETT). *Radiology* 114:89-98, 1975
2. Vitor T, Martins KM, Ionescu TM, et al: PET/MRI: a novel hybrid imaging technique. Major clinical indications and preliminary experience in Brazil. *Einstein (Sao Paulo)* 15:115-118, 2017
3. Lamaka K, Farwell MD, Ichise M: Positron emission tomography. *Handb Clin Neurol* 135:209-227, 2016
4. Slates RB, Farahani K, Shao Y, et al: A study of artefacts in simultaneous PET and MR imaging using a prototype MR compatible PET scanner. *Phys Med Biol* 44:2015-2027, 1999
5. Varrone A, Asenbaum S, Borghat TV, et al: EANM procedure guidelines for PET brain imaging using [ $^{18}\text{F}$ ]FDG, version 2. *Eur J Nucl Med Mol Imaging* 36:2103-2110, 2009
6. Catana C, Wu Y, Judenhofer MS, et al: Simultaneous acquisition of multislice PET and MR images: initial results with a MR-compatible PET scanner. *J Nucl Med* 47:1968-1976, 2006
7. Yang ZL, Zhang LJ: PET/MRI of central nervous system: current status and future perspective. *Eur Radiol* 26:3534-3541, 2016
8. Spick C, Herrmann K, Czernin J:  $^{18}\text{F}$ -FDG PET/CT and PET/MRI perform equally well in cancer: evidence from studies on more than 2,300 patients. *J Nucl Med* 57:420-430, 2016
9. Engert A, Haverkamp H, Kobe C, et al: Reduced-intensity chemotherapy and PET-guided radiotherapy in patients with advanced stage Hodgkin's lymphoma (HD15 trial): a randomised, open-label, phase 3 non-inferiority trial. *Lancet* 379:1791-1799, 2012
10. Glaudemans AW, Quintero AM, Signore A: PET/MRI in infectious and inflammatory diseases: will it be a useful improvement? *Eur J Nucl Med Mol Imaging* 39:745-749, 2012
11. Marzola P, Osculati F, Sbarbati A: High field MRI in preclinical research. *Eur J Radiol* 48:165-170, 2003
12. Hong YH, Kong EJ:  $^{18}\text{F}$ Fluoro-deoxy-D-glucose uptake of knee joints in the aspect of age-related osteoarthritis: A case-control study. *BMC Musculoskelet Disord* 14:141, 2013
13. Kubota R, Yamada S, Kubota K, et al: Intratumoral distribution of fluorine-18-fluorodeoxyglucose in vivo: High accumulation in macrophages and granulation tissues studied by microautoradiography. *J Nucl Med* 33:1972-1980, 1992
14. Brewer S, McPherson M, Fujiwara D, et al: Molecular imaging of murine intestinal inflammation with 2-deoxy-2- [ $^{18}\text{F}$ ]fluoro-D-glucose and positron emission tomography. *Gastroenterology* 135:744-755, 2008
15. Blau M, Nagler W, Bender MA: Fluorine-18: A new isotope for bone scanning. *J Nucl Med* 3:332-334, 1962
16. Czernin J, Satyramurthy N, Schiepers C: Molecular mechanisms of bone  $^{18}\text{F}$ -NaF deposition. *J Nucl Med* 51:1826-1829, 2010

17. Schiepers C, Nuyts J, Bormans G, et al: Fluoride kinetics of the axial skeleton measured in vivo with fluorine-18-fluoride PET. *J Nucl Med* 38:1970-1976, 1997
18. Kobayashi N, Inaba Y, Tateishi U, et al: New application of 18F-fluoride PET for the detection of bone remodeling in early-stage osteoarthritis of the hip. *Clin Nucl Med* 38:e379-e383, 2013
19. Irkle A, Vesey AT, Lewis DY, et al: Identifying active vascular microcalcification by (18)F-sodium fluoride positron emission tomography. *Nat Commun* 6:7495, 2015
20. Derlin T, Richter U, Bannas P, et al: Feasibility of 18F-sodium fluoride PET/CT for imaging of atherosclerotic plaque. *J Nucl Med* 51:862-865, 2010
21. Naghavi M, Libby P, Falk E, et al: From vulnerable plaque to vulnerable patient: A call for new definitions and risk assessment strategies: Part I. *Circulation* 108:1664-1672, 2003
22. Naghavi M, Libby P, Falk E, et al: From vulnerable plaque to vulnerable patient: a call for new definitions and risk assessment strategies: Part II. *Circulation* 108:1772-1778, 2003
23. Alie N, Eldib M, Fayad ZA, et al: Inflammation, atherosclerosis, and coronary artery disease: PET/CT for the evaluation of atherosclerosis and inflammation. *Clin Med Insights Cardiol*. 8:13-21, 2014 (suppl 3)
24. Evans NR, Tarkin JM, Chowdhury MM, et al: PET imaging of atherosclerotic disease: advancing plaque assessment from anatomy to pathophysiology. *Curr Atheroscler Rep* 18:30, 2016
25. Wu C, Ma G, Li J, et al: In vivo cell tracking via (1)(8)F-fluorodeoxyglucose labeling: A review of the preclinical and clinical applications in cell-based diagnosis and therapy. *Clin Imaging* 37:28-36, 2013
26. Adonai N, Nguyen KN, Walsh J, et al: Ex vivo cell labeling with <sup>64</sup>Cu-pyruvaldehyde-bis(N4-methylthiosemicarbazone) for imaging cell trafficking in mice with positron-emission tomography. *Proc Natl Acad Sci USA* 99:3030-3035, 2002
27. Pala A, Liberatore M, D'Elia P, et al: Labelling of granulocytes by phagocytic engulfment with <sup>64</sup>Cu-labelled chitosan-coated magnetic nanoparticles. *Mol Imaging Biol* 14:593-598, 2012
28. Li ZB, Chen K, Wu Z, et al: <sup>64</sup>Cu-labeled PEGylated polyethylenimine for cell trafficking and tumor imaging. *Mol Imaging Biol* 11:415-423, 2009
29. Bhargava KK, Gupta RK, Nichols KJ, et al: In vitro human leukocyte labeling with (<sup>64</sup>Cu): an intraindividual comparison with (111)In-oxine and (18)F-FDG. *Nucl Med Biol*. 36:545-549, 2009
30. Keliher EJ, Yoo J, Nahrendorf M, et al: <sup>89</sup>Zr-labeled dextran nanoparticles allow in vivo macrophage imaging. *Bioconjug Chem* 22:2383-2389, 2011
31. Charoenphun P, Meszaros LK, Chuamsaamarkkee K, et al: <sup>89</sup>Zr]oxinate<sup>4</sup> for long-term in vivo cell tracking by positron emission tomography. *Eur J Nucl Med Mol Imaging* 42:278-287, 2015
32. Fairclough M, Prenant C, Ellis B, et al: A new technique for the radiolabelling of mixed leukocytes with zirconium-89 for inflammation imaging with positron emission tomography. *J Labelled Comp Radiopharm* 59:270-276, 2016
33. Zhu Z, Yin Y, Zheng K, et al: Evaluation of synovial angiogenesis in patients with rheumatoid arthritis using (6)(8)Ga-PRGD2 PET/CT: A prospective proof-of-concept cohort study. *Ann Rheum Dis* 73:1269-1272, 2014
34. Bouter C, Meller B, Sahlmann CO, et al: Imaging chemokine receptor CXCR4 in chronic infection of the bone with (68)Ga-Pentixafor-PET/CT—first insights. *J Nucl Med* 2017, doi:10.2967/jnumed.117.193854
35. Verweij NBS, Gent Y, Huisman M, et al: Rheumatoid arthritis imaging on PET-CT using a novel folate receptor ligand for macrophage targeting [abstract]. *Arthritis Rheumatol* 69:2017 (suppl 10), <http://acrabstracts.org/abstract/rheumatoid-arthritis-imaging-on-pet-ct-using-a-novel-folate-receptor-ligand-for-macrophage-targeting/>. Accessed January 7, 2018
36. Xia W, Hilgenbrink AR, Matteson EL, et al: A functional folate receptor is induced during macrophage activation and can be used to target drugs to activated macrophages. *Blood* 113:438-446, 2009
37. Diaz LA Jr, Foss CA, Thornton K, et al: Imaging of musculoskeletal bacterial infections by [<sup>124</sup>I]FIAU-PET/CT. *PLoS ONE* 2:2007, e1007
38. Zhang XM, Zhang HH, McLeroth P, et al: [<sup>124</sup>I]FIAU: Human dosimetry and infection imaging in patients with suspected prosthetic joint infection. *Nucl Med Biol*. 43:273-279, 2016
39. Venneti S, Lopresti BJ, Wiley CA: The peripheral benzodiazepine receptor (Translocator protein 18 kDa) in microglia: From pathology to imaging. *Prog Neurobiol* 80:308-322, 2006
40. Tronel C, Largeau B, Santiago Ribeiro MJ, et al: Molecular targets for PET imaging of activated microglia: The current situation and future expectations. *Int J Mol Sci* 18:802, 2017
41. van Oosten M, Hahn M, Crane LM, et al: Targeted imaging of bacterial infections: advances, hurdles and hopes. *FEMS Microbiol Rev* 39:892-916, 2015
42. Ordonez AA, Weinstein EA, Bambarger LE, et al: A systematic approach for developing bacteria-specific imaging tracers. *J Nucl Med* 58:144-150, 2017
43. Weinstein EA, Ordonez AA, DeMarco VP, et al: Imaging enterobacteriaceae infection in vivo with 18F-fluorodeoxyisorbital positron emission tomography. *Sci Transl Med* 6:259ra146, 2014
44. Zhu W, Yao S, Xing H, et al: Biodistribution and radiation dosimetry of the enterobacteriaceae-specific imaging probe [(18)F]fluorodeoxyisorbital determined by PET/CT in healthy human volunteers. *Mol Imaging Biol* 18:782-787, 2016
45. Lee HY, Li Z, Chen K, et al: PET/MRI dual-modality tumor imaging using arginine-glycine-aspartic (RGD)-conjugated radiolabeled iron oxide nanoparticles. *J Nucl Med* 49:1371-1379, 2008
46. Zhu H, Zhao J, Lin X, et al: Design, synthesis and evaluation of dual-modality glyco-nanoparticles for tumor imaging. *Molecules* 18:6425-6438, 2013
47. Uppal R, Catana C, Ay I, et al: Bimodal thrombus imaging: Simultaneous PET/MR imaging with a fibrin-targeted dual PET/MR probe—feasibility study in rat model. *Radiology* 258:812-820, 2011
48. Yang X, Hong H, Grailer JJ, et al: cRGD-functionalized, DOX-conjugated, and (6)(4)Cu-labeled superparamagnetic iron oxide nanoparticles for targeted anticancer drug delivery and PET/MR imaging. *Biomaterials* 32:4151-4160, 2011
49. Vecchione D, Aiello M, Cavaliere C, et al: Hybrid core shell nanoparticles entrapping Gd-DTPA and (18)F-FDG for simultaneous PET/MRI acquisitions. *Nanomedicine (Lond)* 12:2223-2231, 2017
50. Lahooti A, Sarkar S, Laurent S, Shanehazzadeh S. Dual nano-sized contrast agents in PET/MRI: A systematic review. *Contrast Media Mol Imaging* 11:428-447, 2016
51. Garibotto V, Heinzer S, Vulliemoz S, et al: Clinical applications of hybrid PET/MRI in neuroimaging. *Clin Nucl Med* 38:e13-e18, 2013
52. Hitz S, Habekost C, Furst S, et al: Systematic comparison of the performance of integrated whole-body PET/MR imaging to conventional PET/CT for (1)(8)F-FDG brain imaging in patients examined for suspected dementia. *J Nucl Med* 55:923-931, 2014
53. Day BK, Eisenman L, Black J, et al: A case study of voltage-gated potassium channel antibody-related limbic encephalitis with PET/MRI findings. *Epilepsy Behav Case Rep* 4:23-26, 2015
54. Jolepalem P, Wong CY: Neurocysticercosis on 18F-FDG PET/MRI: Co-registered Images. *Clin Nucl Med* 39:e110-e113, 2014
55. Taneja S, Jena A, Kaul S, et al: Somatostatin receptor-positive granulomatous inflammation mimicking as meningioma on simultaneous PET/MRI. *Clin Nucl Med* 40:e71-e72, 2015
56. Kaur G, Cameron L, Syrityna O, et al: A case report of neurosarcoidosis presenting as a lymphoma mimic. *Case Rep Neurol Med* 2016:7464587, 2016
57. Rocchi L, Niccolini F, Politis M: Recent imaging advances in neurology. *J Neurol* 262:2182-2194, 2015
58. Bolcaen J, Acou M, Mertens K, et al: Structural and metabolic features of two different variants of multiple sclerosis: A PET/MRI study. *J Neuroimaging* 23:431-436, 2013

59. Grecchi E, Veronese M, Bodini B, et al: Multimodal partial volume correction: Application to [(11)C]PIB PET/MRI myelin imaging in multiple sclerosis. *J Cereb Blood Flow Metab* 37:3803-3817, 2017
60. Vezzani A, Aronica E, Mazarati A, et al: Epilepsy and brain inflammation. *Exp Neurol* 244:11-21, 2013
61. Bogdanovic RM, Syvanen S, Michler C, et al: R)-[11C]PK11195 brain uptake as a biomarker of inflammation and antiepileptic drug resistance: Evaluation in a rat epilepsy model. *Neuropharmacology* 85:104-112, 2014
62. Matthews PM, Datta G: Positron-emission tomography molecular imaging of glia and myelin in drug discovery for multiple sclerosis. *Expert Opin Drug Discov* 10:557-570, 2015
63. Whittington RA, Planel E, Terrando N: Impaired Resolution of Inflammation in Alzheimer's Disease: A Review. *Front Immunol* 8:1464, 2017
64. Salter MW, Stevens B: Microglia emerge as central players in brain disease. *Nat Med* 23:1018-1027, 2017
65. Bagyinszky E, Giau VV, Shim K, et al: Role of inflammatory molecules in the Alzheimer's disease progression and diagnosis. *J Neurol Sci* 376:242-254, 2017
66. Joshi N, Singh S: Updates on immunity and inflammation in Parkinson disease pathology. *J Neurosci Res* 2017, doi:10.1002/jnr.24185
67. Harhausen D, Sudmann V, Khojasteh U, et al: Specific imaging of inflammation with the 18 kDa translocator protein ligand DPA-714 in animal models of epilepsy and stroke. *PLoS ONE* 8:2013, e69529
68. Park E, Gallezot JD, Delgado A, et al: 11C-PBR28 imaging in multiple sclerosis patients and healthy controls: Test-retest reproducibility and focal visualization of active white matter areas. *Eur J Nucl Med Mol Imaging* 42:1081-1092, 2015
69. Banati RB, Newcombe J, Gunn RN, et al: The peripheral benzodiazepine binding site in the brain in multiple sclerosis: Quantitative in vivo imaging of microglia as a measure of disease activity. *Brain* 123(Pt 11):2321-2337, 2000
70. Pappata S, Levasseur M, Gunn RN, et al: Thalamic microglial activation in ischemic stroke detected in vivo by PET and [11C]PK1195. *Neurology* 55:1052-1054, 2000
71. Yasuno F, Ota M, Kosaka J, et al: Increased binding of peripheral benzodiazepine receptor in Alzheimer's disease measured by positron emission tomography with [11C]DAA1106. *Biol Psychiatry* 64:835-841, 2008
72. Ramlackhansingh AF, Brooks DJ, Greenwood RJ, et al: Inflammation after trauma: Microglial activation and traumatic brain injury. *Ann Neurol* 70:374-383, 2011
73. Du J, Takahashi AM, Chung CB: Ultrashort TE spectroscopic imaging (UTESI): Application to the imaging of short T2 relaxation tissues in the musculoskeletal system. *J Magn Reson Imaging* 29:412-421, 2009
74. Welsch GH, Mamisch TC, Hughes T, et al: In vivo biochemical 7.0 Tesla magnetic resonance: Preliminary results of dGEMRIC, zonal T2, and T2\* mapping of articular cartilage. *Invest Radiol* 43:619-626, 2008
75. Singh A, Haris M, Cai K, et al: High resolution T1 $\rho$  mapping of in vivo human knee cartilage at 7T. *PLoS ONE* 9:2014, e97486
76. Staroswiecki E, Granlund KL, Alley MT, et al: Simultaneous estimation of T(2) and apparent diffusion coefficient in human articular cartilage in vivo with a modified three-dimensional double echo steady state (DESS) sequence at 3 T. *Magn Reson Med* 67:1086-1096, 2012
77. Englund EK, Rodgers ZB, Langham MC, et al: Measurement of skeletal muscle perfusion dynamics with pseudo-continuous arterial spin labeling (pCASL): Assessment of relative labeling efficiency at rest and during hyperemia, and comparison to pulsed arterial spin labeling (PASL). *J Magn Reson Imaging* 44:929-939, 2016
78. Kogan F, Haris M, Singh A, et al: Method for high-resolution imaging of creatine in vivo using chemical exchange saturation transfer. *Magn Reson Med* 71:164-172, 2014
79. Kogan F, Haris M, Debrosse C, et al: In vivo chemical exchange saturation transfer imaging of creatine (CrCEST) in skeletal muscle at 3T. *J Magn Reson Imaging* 40:596-602, 2014
80. Damon BM, Froeling M, Buck AK, et al: Skeletal muscle diffusion tensor-MRI fiber tracking: Rationale, data acquisition and analysis methods, applications and future directions. *NMR Biomed* 30:e3563, 2017
81. Chu CR, Williams AA, West RV, et al: Quantitative magnetic resonance imaging UTE-T2\* mapping of cartilage and meniscus healing after anatomic anterior cruciate ligament reconstruction. *Am J Sports Med* 42:1847-1856, 2014
82. Du J, Bydder M, Takahashi AM, et al: Short T2 contrast with three-dimensional ultrashort echo time imaging. *Magn Reson Imaging* 29:470-482, 2011
83. Chen K, Blebea J, Laredo JD, et al: Evaluation of musculoskeletal disorders with PET, PET/CT, and PET/MR imaging. *PET Clin.* 3:451-465, 2008
84. Kogan F, Fan AP, McWalter EJ, et al: PET/MRI of metabolic activity in osteoarthritis: A feasibility study. *J Magn Reson Imaging* 45:1736-1745, 2017
85. Buchbender C, Ostendorf B, Ruhlmann V, et al: Hybrid 18F-labeled Fluoride Positron Emission Tomography/Magnetic Resonance (MR) imaging of the sacroiliac joints and the spine in patients with axial spondyloarthritis: A pilot study exploring the link of mr bone pathologies and increased osteoblastic activity. *J Rheumatol* 42:1631-1637, 2015
86. Rosado-de-Castro PH, Lopes de Souza SA, Alexandre D, et al: Gutflin B. Rheumatoid arthritis: Nuclear medicine state-of-the-art imaging. *World J Orthop* 5:312-318, 2014
87. Miese F, Scherer A, Ostendorf B, et al: Hybrid 18F-FDG PET-MRI of the hand in rheumatoid arthritis: Initial results. *Clin Rheumatol* 30:1247-1250, 2011
88. Chaudhari AJ, Bowen SL, Burkett GW, et al: High-resolution (18)F-FDG PET with MRI for monitoring response to treatment in rheumatoid arthritis. *Eur J Nucl Med Mol Imaging* 37:1047, 2010
89. Biniiecka M, Canavan M, McGarry T, et al: Dysregulated bioenergetics: A key regulator of joint inflammation. *Ann Rheum Dis* 75:2192-2200, 2016
90. Fuchs K, Kuehn A, Mahling M, et al: In vivo hypoxia PET imaging quantifies the severity of arthritic joint inflammation in line with overexpression of hypoxia-inducible factor and enhanced reactive oxygen species generation. *J Nucl Med* 58:853-860, 2017
91. Fahnert J, Purz S, Jarvers JS, et al: Use of simultaneous 18F-FDG PET/MRI for the detection of spondylodiskitis. *J Nucl Med* 57:1396-1401, 2016
92. Basu S, Zhuang H, Alavi A: FDG PET and PET/CT imaging in complicated diabetic foot. *PET Clin.* 7:151-160, 2012
93. Rao H, Gaur N, Tipre D: Assessment of diabetic neuropathy with emission tomography and magnetic resonance spectroscopy. *Nucl Med Commun* 38:275-284, 2017
94. Chaudhry AA, Gul M, Gould E, et al: Utility of positron emission tomography-magnetic resonance imaging in musculoskeletal imaging. *World J Radiol* 8:268-274, 2016
95. Manabe O, Yoshinaga K, Ohira H, et al: The effects of 18-h fasting with low-carbohydrate diet preparation on suppressed physiological myocardial (18)F-fluorodeoxyglucose (FDG) uptake and possible minimal effects of unfractionated heparin use in patients with suspected cardiac involvement sarcoidosis. *J Nucl Cardiol* 23:244-252, 2016
96. Williams G, Kolodny GM: Suppression of myocardial 18F-FDG uptake by preparing patients with a high-fat, low-carbohydrate diet. *AJR Am J Roentgenol* 190:W151-W156, 2008
97. Nensa F, Tezga E, Schweins K, et al: Evaluation of a low-carbohydrate diet-based preparation protocol without fasting for cardiac PET/MR imaging. *J Nucl Cardiol* 24:980-988, 2017
98. Writing g, Document reading g, for ERTdwrbmotESDC: A joint procedural position statement on imaging in cardiac sarcoidosis: From the Cardiovascular and Inflammation & Infection Committees of the European Association of Nuclear Medicine, the European Association of Cardiovascular Imaging, and the American Society of Nuclear Cardiology. *Eur Heart J Cardiovasc Imaging* 18:1073-1089, 2017



99. Prieto-González S, García-Martínez A, Tavera-Bahillo I, et al: Effect of glucocorticoid treatment on computed tomography angiography detected large-vessel inflammation in giant-cell arteritis. A prospective, longitudinal study. *Medicine (Baltimore)* 94:e486, 2015
100. Nielsen BDTHL, Keller KK, Therkildsen P, et al: Attenuation of Fluorine-18-fluorodeoxyglucose uptake in large vessel giant cell arteritis after short-term high-dose steroid treatment—a diagnostic window of opportunity. *Arthritis Rheumatol* 68:2016 (suppl 10), abstract
101. Ouyang J, Li Q, El Fakhri G: Magnetic resonance-based motion correction for positron emission tomography imaging. *Semin Nucl Med* 43:60-67, 2013
102. Munoz C, Kolbitsch C, Reader AJ, et al: MR-Based Cardiac and Respiratory Motion-Compensation Techniques for PET-MR Imaging. *PET Clin.* 11:179-191, 2016
103. Le Meunier L, Slomka PJ, Dey D, et al: Motion frozen (18)F-FDG cardiac PET. *J Nucl Cardiol* 18:259-266, 2011
104. Feng T, Wang J, Fung G, et al: Non-rigid dual respiratory and cardiac motion correction methods after, during, and before image reconstruction for 4D cardiac PET. *Phys Med Biol* 61:151-168, 2016
105. Kolbitsch C, Ahlman MA, Davies-Venn C, et al: Cardiac and Respiratory Motion Correction for Simultaneous Cardiac PET/MR. *J Nucl Med* 58:846-852, 2017
106. Beyer T, Lassen ML, Boellaard R, et al: Investigating the state-of-the-art in whole-body MR-based attenuation correction: An intra-individual, inter-system, inventory study on three clinical PET/MR systems. *MAGMA* 29:75-87, 2016
107. Vontobel J, Liga R, Possner M, et al: MR-based attenuation correction for cardiac FDG PET on a hybrid PET/MRI scanner: Comparison with standard CT attenuation correction. *Eur J Nucl Med Mol Imaging* 42:1574-1580, 2015
108. Ishida Y, Yoshinaga K, Miyagawa M, et al: Recommendations for (18)F-fluorodeoxyglucose positron emission tomography imaging for cardiac sarcoidosis: Japanese Society of Nuclear Cardiology recommendations. *Ann Nucl Med* 28:393-403, 2014
109. Larici AR, Glaudemans AW, Del Ciello A, et al: Radiological and nuclear medicine imaging of sarcoidosis. *Q J Nucl Med Mol Imaging* 2017, doi:10.23736/S1824-4785.17.03046-1
110. Birnie DH, Sauer WH, Bogun F, et al: HRS expert consensus statement on the diagnosis and management of arrhythmias associated with cardiac sarcoidosis. *Heart Rhythm* 11:1305-1323, 2014
111. Ohira H, Birnie DH, Pena E, et al: Comparison of (18)F-fluorodeoxyglucose positron emission tomography (FDG PET) and cardiac magnetic resonance (CMR) in corticosteroid-naïve patients with conduction system disease due to cardiac sarcoidosis. *Eur J Nucl Med Mol Imaging* 43:259-269, 2016
112. Abgral R, Dweck MR, Trivieri MG, et al: Clinical utility of combined FDG-PET/MR to assess myocardial disease. *JACC Cardiovasc Imaging.* 10:594-597, 2017
113. Wada K, Niitsuma T, Yamaki T, et al: Simultaneous cardiac imaging to detect inflammation and scar tissue with (18)F-fluorodeoxyglucose PET/MRI in cardiac sarcoidosis. *J Nucl Cardiol* 23:1180-1182, 2016
114. Dweck MR, Abgral R, Trivieri MG, et al: Hybrid magnetic resonance imaging and positron emission tomography with fluorodeoxyglucose to diagnose active cardiac sarcoidosis. *JACC Cardiovasc Imaging.* 11:94-107, 2018
115. Nensa F, Tezgh E, Poeppel T, et al: Diagnosis and treatment response evaluation of cardiac sarcoidosis using positron emission tomography/magnetic resonance imaging. *Eur Heart J* 36:550, 2015
116. Osborne MT, Hulten EA, Singh A, et al: Reduction in <sup>18</sup>F-fluorodeoxyglucose uptake on serial cardiac positron emission tomography is associated with improved left ventricular ejection fraction in patients with cardiac sarcoidosis. *J Nucl Cardiol* 21:166-174, 2014
117. Gormsen LC, Haraldsen A, Kramer S, et al: A dual tracer (68)Ga-DOTANOC PET/CT and (18)F-FDG PET/CT pilot study for detection of cardiac sarcoidosis. *EJNMMI Res* 6:52, 2016
118. Slart RHJA, Koopmans KP, van Geel PP, et al: Somatostatin receptor based hybrid imaging. Short communication. *Eur Hybrid J, MM Imaging* 1:7, 2017, in press
119. Lurz P, Luecke C, Eitel I, et al: Comprehensive cardiac magnetic resonance imaging in patients with suspected myocarditis: The myoracer-trial. *J Am Coll Cardiol* 67:1800-1811, 2016
120. Friedrich MG, Sechtem U, Schulz-Menger J, et al: Cardiovascular magnetic resonance in myocarditis: A JACC White Paper. *J Am Coll Cardiol* 53:1475-1487, 2009
121. Nensa F, Kloth J, Tezgh E, et al: Feasibility of FDG-PET in myocarditis: Comparison to CMR using integrated PET/MRI. *J Nucl Cardiol* 1-10, 2016
122. von Olshausen G, Hyafil F, Langwieser N, et al: Detection of acute inflammatory myocarditis in Epstein Barr virus infection using hybrid 18F-fluoro-deoxyglucose-positron emission tomography/magnetic resonance imaging. *Circulation* 130:925-926, 2014
123. Maya Y, Werner RA, Schütz C, et al: 11C-methionine PET of myocardial inflammation in a rat model of experimental autoimmune myocarditis. *J Nucl Med* 57:1985-1990, 2016
124. Jennette JC, Falk RJ, Bacon PA, et al: 2012 revised International Chapel Hill Consensus Conference Nomenclature of Vasculitides. *Arthritis Rheum* 65:1-11, 2013
125. Maksimowicz-McKinnon K, Clark TM, Hoffman GS: Takayasu arteritis and giant cell arteritis: A spectrum within the same disease? *Medicine (Baltimore)* 88:221-226, 2009
126. Einspieler I, Thürmel K, Pyka T, et al: Imaging large vessel vasculitis with fully integrated PET/MRI: a pilot study. *Eur J Nucl Med Mol Imaging* 42:1012-1024, 2015
127. Riemer HJA, Slart AWJMG, Chareonthaitawee P, et al: FDG-PET/CT(A) imaging in large vessel vasculitis and polymyalgia rheumatica: Joint procedural recommendation of the EANM, SNMMI, the PET Interest Group (PIG), and endorsed by the ASNC. *Eur J Nucl Med Mol Imaging* 2018, In press
128. Maccioni F, Patak MA, Signore A, et al: New frontiers of MRI in Crohn's disease: Motility imaging, diffusion-weighted imaging, perfusion MRI, MR spectroscopy, molecular imaging, and hybrid imaging (PET/MRI). *Abdom Imaging* 37:974-982, 2012
129. Anupindi SA, Grossman AB, Nimkin K, et al: Imaging in the evaluation of the young patient with inflammatory bowel disease: What the gastroenterologist needs to know. *J Pediatr Gastroenterol Nutr* 59:429-439, 2014
130. Lichtenstein GR, Rutgeerts P: Importance of mucosal healing in ulcerative colitis. *Inflamm Bowel Dis* 16:338-346, 2010
131. Shih IL, Wei SC, Yen RF, et al: PET/MRI for evaluating subclinical inflammation of ulcerative colitis. *J Magn Reson Imaging* 2017, doi:10.1002/jmri.25795
132. Maccioni F, Colaiacomo MC, Parlanti S: Ulcerative colitis: Value of MR imaging. *Abdom Imaging* 30:584-592, 2005
133. Klang E, Kopylov U, Eliakim R, et al: Diffusion-weighted imaging in quiescent Crohn's disease: Correlation with inflammatory biomarkers and video capsule endoscopy. *Clin Radiol* 72:798 e7-e13, 2017
134. Zhang J, Li LF, Zhu YJ, et al: Diagnostic performance of 18F-FDG-PET versus scintigraphy in patients with inflammatory bowel disease: A meta-analysis of prospective literature. *Nucl Med Commun* 35:1233-1246, 2014
135. Catalano OA, Gee MS, Nicolai E, et al: Evaluation of quantitative PET/MR enterography biomarkers for discrimination of inflammatory strictures from fibrotic strictures in crohn disease. *Radiology* 278:792-800, 2016
136. Pellino G, Nicolai E, Catalano OA, et al: PET/MR versus PET/CT imaging: Impact on the Clinical management of small-bowel crohn's disease. *J Crohns Colitis* 10:277-285, 2016
137. Thuermel K, Einspieler I, Wolfram S, et al: Disease activity and vascular involvement in retroperitoneal fibrosis: First experience with fully integrated 18F-fluorodeoxyglucose positron emission tomography/magnetic resonance imaging compared to clinical and laboratory parameters. *Clin Exp Rheumatol* 103:146-154, 2017, 35 Suppl
138. Lotsch F, Waneck F, Auer H, et al: FDG-PET/MRI in alveolar echinococcosis. *Int J Infect Dis* 64:67-68, 2017
139. Gatidis S, Schmidt H, Gucke B, et al: Comprehensive oncologic imaging in infants and preschool children with substantially reduced radiation

exposure using combined simultaneous (1)(8)f-fluorodeoxyglucose positron emission tomography/magnetic resonance imaging: A direct comparison to (1)(8)f-fluorodeoxyglucose positron emission tomography/computed tomography. *Invest Radiol* 51:7-14, 2016

140. Muehe AM, Theruvath AJ, Lai L, et al: How to provide gadolinium-free pet/mr cancer staging of children and young adults in less than 1 h: The stanford approach. *Mol Imaging Biol* 2017, doi:10.1007/s11307-017-1105-7